

1 **Genomic selection for resistance to one pathogenic strain of *Vibrio splendidus***
2 **in blue mussel *Mytilus edulis***

3 **Munusamy Ajithkumar¹⁺, Jonathan D'Ambrosio², Marie-Agnès Travers³, Romain**
4 **Morvezen^{2*}, Lionel Degremont^{1*}**

5

6 ¹Ifremer ASIM, avenue Mus de Loup, 17390 La Tremblade, France

7 ²SYSAAF, Station LPGP/INRAE, Campus de Beaulieu, Rennes 35042, France

8 ³IHPE, Université de Montpellier, CNRS, Ifremer, Univ Perpignan Via Domitia, Montpellier,
9 France

10

11 * Romain Morvezen and Lionel Dégrement contributed equally to this work and should both be considered as last co-authors

12 *Corresponding author: Munusamy Ajithkumar (ajithkumar.munusamy@ifremer.fr)

13

14

15

16

17 **Highlights**

- 18 - Moderate heritability was observed for resistance to *Vibrio splendidus*
- 19 - Genomic selection has better prediction accuracy than pedigree-based
20 selection
- 21 - Resistance to *V. splendidus* is a polygenic trait

22

23

24

25

26

27

28

29 **Abstract**

30 The blue mussel is one of the major aquaculture species worldwide. In France, this
31 species faces a significant threat from infectious disease outbreaks in both mussel
32 farms and the natural environment over the past decade. Diseases caused by various
33 pathogens, particularly *Vibrio* spp., have posed a significant challenge to the mussel
34 industry. Genetic improvement of disease resistance can be an effective approach to
35 overcoming this issue. In this work, we tested genomic selection (GS) in the blue
36 mussel (*Mytilus edulis*) to understand the genetic basis of resistance to one pathogenic
37 strain of *Vibrio splendidus* (strain 14/053 2T1) and to predict the accuracy of selection
38 using both pedigree and genomic information. Additionally, we performed a genome-
39 wide association study (GWAS) to identify putative QTLs underlying disease
40 resistance. We conducted an experimental infection involving 2,160 mussels sampled
41 from 24 half-sib families containing each two full-sib families which were injected with
42 *V. splendidus*. Dead and survivors mussels were all sampled, and among them, 348
43 dead and 348 surviving mussels were genotyped using a recently published multi-
44 species medium-density 60K SNP array. From potentially 23.5K SNPs for *M. edulis*
45 present on the array, we identified 3,404 high-quality SNPs, out of which 2,204 SNPs
46 were successfully mapped onto the recently published reference genome. Heritability
47 for resistance to *V. splendidus* was moderate ranging from 0.22 to 0.31 for a pedigree-
48 based model and from 0.28 to 0.36 for a genomic-based model. GWAS revealed the
49 polygenic architecture of the resistance trait in the blue mussel. The GS models studied
50 showed overall better performance than the pedigree-based model in terms of
51 accuracy of breeding values prediction. This work provides insights into the genetic
52 basis of resistance to *V. splendidus* and exemplifies the potential of genomic selection
53 in family-based breeding programs in *M. edulis*.

54 *Keywords:* Mussels, Mortality, Breeding program, Prediction accuracy, GWAS,
55 Linkage disequilibrium, *Vibrio*

56

57

58 **1. Introduction**

59 Aquaculture is a rapidly growing food production industry globally, supplying
60 over 50% of aquatic protein sources and having a lower carbon footprint compared to
61 terrestrial animals (Norman et al., 2019). Mussels are one of the major aquaculture
62 species worldwide, with France being the second European producers, with around
63 65,000 tons in 2021 (FAO, 2023). Two species as well as their hybrids are cultivated
64 in France: the blue mussel *Mytilus edulis*, and the Mediterranean mussel *Mytilus*
65 *galloprovincialis*. Production is distributed along the English Channel to the southwest
66 coastline of France, and Mediterranean shores (FAO, 2023; Prou and Gouletquer,
67 2002). This species has been widely cultured due to its strong environmental
68 adaptability, high nutritious value, and consumer preference (Prou and Gouletquer,
69 2002; Suplicy, 2020). French mussel production entirely relies on wild spat collection,
70 mainly in Pays de Loire and in Nouvelle-Aquitaine regions (Prou and Gouletquer,
71 2002). Consequently, the French cultivated mussels are not genetically selected
72 through selective breeding programs.

73 Recurrent mass mortality outbreaks of bivalves reduce production, cause
74 economic losses, and negatively impact the ecosystem of natural bivalve populations
75 as well as terrestrial food web (Bódis et al., 2014; Soon and Ransangan, 2019). Mass
76 mortality of various cultured mussels have been reported worldwide such as in blue
77 mussels (Capelle et al., 2021; Lupo et al., 2021), Mediterranean mussels (Avdelas et

78 al., 2021; Lupo et al., 2021), green-lipped mussels (Ericson et al., 2023), and
79 pheasantshell mussels (Putnam et al., 2023), and their occurrence seems to increase
80 in the context of global warming. Since 2014, French mussel farms have been
81 vulnerable to abnormal mussel mortality (AMM) with a mortality rate varying from 30 to
82 100% depending on sites, years or seasons (Normand et al., 2022; Polsenaere et al.,
83 2017). Peak of mortality outbreaks generally occurs during spring (Charles et al.,
84 2020a; Degremont et al., 2019). Various studies are being conducted to identify the
85 cause(s) of AMM outbreaks in France and to propose solutions for reducing mass
86 mortalities in mussel farms and wild stocks. Until now, the etiology of AMM outbreaks
87 remains unclear, but it could be linked to environmental pollutions, seawater
88 characteristics, mussel characteristics, culture practices, and climate change (Lupo et
89 al., 2021; Polsenaere et al., 2017). Pathogens could also be involved in mortality
90 outbreaks, with the pathogenic bacteria *Vibrio splendidus* being found in large
91 abundance in moribund mussels during AMM outbreaks (Bechemin et al., 2015; Ben
92 Cheikh et al., 2016) . *V. splendidus* is a complex species comprising multiple strains,
93 ranging from highly virulent to relatively innocuous (Ben Cheikh et al., 2016). Some
94 virulent strains have been shown to be highly pathogenic to blue mussels, causing high
95 mortality rates up to 90% within a week in experimental challenges (Ben Cheikh et al.,
96 2017; Ben Cheikh et al., 2016; Oden et al., 2016). The virulence of these strains can
97 vary based on factors such as mussel physiology, environmental conditions, and
98 seasonal changes (Charles et al., 2020b). While *V. splendidus* is not the direct cause
99 of AMM, its consistent association with mortality outbreaks suggests it may play a
100 contributory role under specific conditions. Recent studies on bivalve immune
101 responses often lack a validated understanding of immune effectors or pathways,

102 reflecting their reliance on innate rather than adaptive immunity, limiting the efficacy of
103 vaccination strategies (Allam and Raftos, 2015; Rey-Campos et al., 2019).

104 Selective breeding could be a useful approach to enhance the innate immune
105 responses in bivalves (Dégremont et al., 2015; Hollenbeck and Johnston, 2018).
106 Understanding genetic basis of disease resistance is critical for its improvement
107 through selective breeding. The potential for genetic improvement through mass
108 selection is well documented in many bivalve species during the past decades,
109 particularly due to their short generation intervals and their high reproductive capacity
110 allowing the possibility of applying high selection pressures (Gjedrem and Rye, 2018;
111 Tan et al., 2020). Mass selection has been carried for growth traits in Chilean blue
112 mussel *Mytilus chilensis* (Toro et al., 2004a; Toro et al., 2004b), and ploidy status for
113 Mediterranean mussel *M. galloprovincialis* (Ajithkumar et al., 2024a). Lately, a mass
114 selection scheme implemented for resistance to AMM outbreaks in the blue mussel *M.*
115 *edulis* resulted in a 34–48% increase in survival after one generation of selection
116 (Degremont et al., 2019). Although mass selection is effective, it may quickly lead to
117 inbreeding if genetic diversity is not properly monitored (Hu et al., 2022). However, as
118 an alternative strategy to individual selection, family based selective breeding
119 programs have been initiated to estimate breeding values by combining phenotypic
120 information and pedigree. These programs have targeted various traits across different
121 mussel species, such as growth in *M. edulis* (Mallet et al., 1986), *M. galloprovincialis*
122 (Díaz-Puente et al., 2020; Nguyen et al., 2014; Pino-Querido et al., 2015), *M. chilensis*
123 (Alcapán et al., 2007; Guíñez et al., 2017), *Hyriopsis cumingii* (Bai et al., 2017; Jin et
124 al., 2012), *Perna calaniticulus* (Camara and Symonds, 2014); shell nacre color in *H.*
125 *cumingii* (Bai et al., 2017); toxin accumulation and mantle color in *M. galloprovincialis*
126 (Pino-Querido et al., 2015); and survival in *M. edulis* (Mallet et al., 1986).

127 Accurate estimations of breeding values are essential for developing a breeding
128 program and predicting the responses of traits of interest to selection. Recent
129 developments of high throughput genotyping technology now enable the
130 implementation of genomic selection (GS) (Boudry et al., 2021). GS is particularly
131 suitable for traits that are expensive or difficult to measure (e.g. resistance to diseases,
132 meat quantity) because less phenotypic data is needed to obtain similar accuracies
133 from estimated breeding values (EBV) resulting from pedigree-based selection (Regan
134 et al., 2021; Yáñez et al., 2023). GS can improve the genetic gain by capturing both
135 within and between family genetic variation components (Boudry et al., 2021). Next-
136 generation sequencing (NGS) and genotyping-by-sequencing (GBS) tools have been
137 developed for oyster, clam, abalone and scallop (Jiao et al., 2014; McCarty et al., 2022;
138 Nie et al., 2017; Ren et al., 2016; Wang et al., 2016; Yang et al., 2022). However, they
139 do not provide the same set of markers from one population to another (e.g. between
140 training population and breeding population) and are dependent on DNA quality, which
141 limits their potential to develop repeatable genomic analyses. Alternatively, SNP arrays
142 have been developed in some commercially important bivalve species such as the
143 silver-lipped pearl oyster *Pinctada maxima*, with an Illumina ~3k iSelect custom array
144 (Jones et al., 2013a), the Pacific oyster (*Crassostrea gigas*), with a 190K SNP array
145 (Qi et al., 2017), the medium density bi-species (Pacific oyster *C. gigas* and European
146 flat oyster *Ostrea edulis*) 57K SNP array (Gutierrez et al., 2017), the Eastern Oyster
147 (*C. virginica*), with a high density 566K and 66K SNP array (Guo et al., 2023), or
148 medium density multi-species (*M. edulis*, *M. galloprovincialis*, *M. trossulus*, and
149 *M. chilensis*) 60K SNP array (Nascimento-Schulze et al., 2023). SNP arrays have been
150 used for various applications in aquaculture species, including identification of genetic
151 architecture of traits, genomic selection (GS), characterization of genetic resources,

152 pedigree monitoring, sex-determination and inbreeding management, but have rarely
153 been used in bivalves (Gutierrez et al., 2020; Jourdan et al., 2023).

154 In aquaculture, the salmon industry has been leading the way in GS for several
155 years (Ajasa et al., 2024; Correa et al., 2017; Odegård et al., 2014; Robledo et al.,
156 2018; Tsai et al., 2015). To date, more and more aquaculture species are following this
157 trend such as rainbow trout, European sea bass, sea bream, Nile tilapia, Channel
158 catfish or whiteleg shrimp (see for review (Boudry et al., 2021; Houston et al., 2020;
159 Song et al., 2022; Yáñez et al., 2023)). The recent development of genotyping tools in
160 bivalves has so far resulted in a relatively limited number of studies on the potential of
161 genomic selection. GS has been investigated in the Portuguese oyster for
162 morphometric traits, edibility traits and disease traits (Vu et al., 2021), in the American
163 oyster for low salinity tolerance (McCarty et al., 2022) and in the silver-lipped oyster for
164 pearl quality traits (Zenger et al., 2019) and growth traits has been studied in the
165 triangle sail mussel (Wang et al., 2022), European flat oyster (Penaloza et al., 2022)
166 and Pacific oyster (Gutierrez et al., 2018; Jourdan et al., 2023). A few studies have
167 been conducted in oysters showing the increase in accuracy of GS over pedigree-
168 based approaches notably for difficult to measure traits, such as disease resistance
169 (Gutierrez et al., 2018; Gutierrez et al., 2020; Jourdan et al., 2023). To date, trials with
170 low-density panels to reduce genomic evaluation costs have been conducted in
171 several aquaculture species, indicating that developing cost-effective strategies for
172 genomic selection will be pivotal in shaping modern aquaculture breeding programs
173 (Penaloza et al., 2022).

174 The aim of our study was to assess the potential of genomic selection for
175 resistance to one pathogenic strain of *V. splendidus* in *M. edulis*. Using a multi-species
176 Axiom Affymetrix 60K SNP array (Nascimento-Schulze et al., 2023), we first

177 characterized the genetic structure and linkage disequilibrium of the blue mussel
178 population. We then estimated genetic parameters for resistance to *V. splendidus* and
179 performed GWAS to investigate its genetic architecture. Finally, we compared the
180 accuracies of genomic selection and pedigree-based selection to provide
181 recommendations for optimizing selective breeding programs.

182

183 **2. Material and Methods**

184 **2.1 Family production**

185 The 48 families of *M. edulis* used in this study are detailly described in
186 (Ajithkumar et al., 2024b). Briefly, three wild mussel populations (OLE-PON, WIM, and
187 YEU_001) were sampled and transferred to the Ifremer hatchery in La Tremblade in
188 the fall of 2016. Each mussel population was cleaned and placed in separate tanks
189 containing unheated UV-treated, and filtered seawater (400 L per hour). To favor
190 gametogenesis, mussels were fed a cultured phytoplankton diet (*Isochrysis galbana*,
191 *Tetraselmis suecica*, and *Skeletonema costatum*). Two sets of crosses were
192 performed in January 2017 (set 1) and in February 2017 (set 2). For each population,
193 100 mussels were individually placed in 400 mL beakers, and spawning was triggered
194 by alternating cold (10°C) and warm seawater (20°C). Depending on the ripeness of
195 the mussels and the sex ratio, 4 males for OLE-PON, and 11 males for YEU_001 were
196 used in set 1, while 9 males were used for WIM in set 2. Within population, each male
197 was mated with two females, producing in total 24 half-sib families, each containing
198 two full-sib families. Each family was grown separately in 30 L tanks filled with filtered
199 and UV-treated seawater at 20°C until the pediveliger stage. Then, downwelling
200 system were used until mussels reached 1 cm. At that size, they were transferred to

201 our nursery in Bouin in April and May 2017 for set 1 and set 2, respectively. For each
202 family, 1000 spat were maintained in 15 L SEAPA© baskets, and all families were
203 raised in a 20 m³ concrete raceway until the start of the experiment, which occurred in
204 July 2018. More detailed on the larval and nursery culture are provided in (Ajithkumar
205 et al., 2024b).

206

207 **2.2 Experimental infection and phenotyping**

208 Detailed step-by-step protocol of the experimental infection is given in
209 Ajithkumar et al. (2024b). Briefly, two experimental infections (EI_1 and EI_2) were
210 conducted in July 2018, each using 24 families randomly sampled among the 48
211 families (mean individual total weight of approximately 5 g). Additionally, a third
212 experimental infection (EI_3) was performed, involving 12 families from each of the
213 first two experiments, to increase the phenotype and genotype sample size. To
214 investigate their resistance to *V. splendidus*, a highly pathogenic strain (strain 14/053
215 2T1) isolated during AMM outbreak in 2014 was injected in 30 mussels per family.
216 First, mussels were anesthetized using MgCl₂ (50 g per L), and 50 µL of bacterial
217 solution (10⁹ bacteria/mL) was injected into the muscle. Then, ten injected mussels per
218 family, for all the 24 families of one set were hold in one 120 L tank containing UV-
219 filtered seawater. Three replicate tanks were used and, in each tank, water
220 recirculation was maintained using a TECO®pump (Ravenna, Italy), which also
221 maintained the seawater temperature at 17°C. Dead mussels were counted and
222 sampled daily up to 72 h post-injection. The adductor muscle/gills of the dead mussels
223 during the experiment and the surviving mussels at the end of the experiment were
224 collected using scalpels disinfected with 70% ethanol and stored in 1.5 ml sterile tubes
225 at room temperature. Individuals for genotyping were randomly sampled from the

226 challenge experiments (EI_1, EI_2, and EI_3), including both dead and alive mussels,
227 with 13 to 16 individuals sampled from each of the 48 families (Table 1).

228

229 **2.3 Genotyping and quality control**

230 Among the 2160 individuals from the 48 families, a total of 768 were sent for
231 DNA extraction and genotyping to the Gentyane INRAE Platform (Clermont-Ferrand,
232 France) using the multi species medium-density 60K SNP-array, Axiom_Myt_v1_r1
233 (Thermo Fisher Scientific, Waltham, Massachusetts, USA), which comprises 23,252
234 markers for *M. edulis* (Nascimento-Schulze et al., 2023). Among the 768 individuals
235 genotyped, 348 were from the dead group, 348 were from the alive group, and the
236 remaining 72 were their parents (48 dams and 24 sires). Quality controls on the 60K
237 SNPs from the SNP array and genotyped individuals were performed as described in
238 D'Ambrosio et al. (2019). Firstly, genotypes of all individuals were analyzed using the
239 Axiom Analysis Suite software (AxAS; v.4.0.3.3) with the default best practice workflow
240 suggested by the manufacturer, with few threshold modifications, which includes
241 individual quality control (QC) and SNP quality control analysis (DQC \geq 0.20; QC call
242 rate \geq 85; percent of passing samples \geq 98; average call rate for passing samples \geq
243 92%; call rate cutoff \geq 95; FLD \geq 2.6). Consequently, 7,476 polymorphic SNPs were
244 retained for further analysis. Subsequently, final quality control was performed using
245 PLINK v1.9 software (Chang et al., 2015). Two individuals with an identity-by-descent
246 value over 0.90 were considered as duplicated and both individuals were removed
247 from the analysis. Only SNPs with a minor allele frequency (MAF) higher than 0.01 and
248 those passing the Hardy-Weinberg equilibrium test (p -value $<$ 0.0000001) in the
249 genotyped mussels were retained. After the quality control, data comprised of a total
250 of 766 genotyped individuals for 3,406 SNPs.

251

252 **2.4 Parentage assignment**

253 Parentage assignment was performed in the R package APIS (Griot et al., 2020)
254 with a mismatch number set to 5%. The best 1471 SNPs (Supplementary Table 1),
255 selected with call rate greater than 90% and MAF value greater than 0.1 were used.
256 Parentage assignment allowed the reconstruction of the pedigree of 647 offspring with
257 assignment rates reaching 93.2% of the mussels having both parents assigned, while
258 the remaining 47 mussels potentially from outside the cross-mating design, which were
259 excluded from following analyses.

260

261 **2.5 Genetic structure of the population**

262 To evaluate potential genetic sub-structuring of populations and any associated
263 biases, a principal component analysis (PCA) was performed using PLINK 1.9 (Chang
264 et al., 2015) and the genetic structure was visualized using in RStudio (Team, 2024).
265 Three individuals were identified as outliers beyond the population structure and were
266 subsequently excluded from further analysis. Genetic differentiation between
267 populations was measured through pairwise fixation index (F_{ST}) estimates using PLINK
268 1.9 (Chang et al., 2015).

269

270 **2.6 SNP mapping, genome coverage and linkage disequilibrium estimation**

271 All markers of the array along with their flanking regions were blasted using a
272 BLASTn® procedure on the reference genome (*Mytilus edulis* genome assembly,
273 xbMytEdu12, GenBank accession number: GCA_963676595.2). To map SNPs,

274 considering the high polymorphism in the mussel genome, four mismatches were
275 allowed over a length of around 71 base pairs. Only SNPs mapping to a unique position
276 on the reference genome were retained for the subsequent stage of quality control as
277 mentioned in previous section. Out of the 3406 SNPs, only 2204 matched our mapping
278 criteria and were successfully positioned on the reference genome (Supplementary
279 Tables 1 & 2).

280 The pairwise linkage disequilibrium (LD) analysis was performed between all
281 SNPs and adjacent markers for each linkage group and population to determine LD
282 decay within the genome of *M. edulis* using Plink 1.9 (Chang et al., 2015).

283

284 **2.7 Estimation of genetic parameters**

285 **2.7.1 PBLUP**

286 Estimated breeding values, variance components, and heritability were
287 calculated using the BLUPF90 software package (Misztal et al., 2014) through two
288 different approaches: a linear mixed model with AIREMLF90 (Misztal et al., 2014) for
289 assessing the trait on the observed scale, and a Gibbs analyses with THRGIBBS1F90
290 (Tsuruta and Misztal, 2006) for evaluating it on the underlying scale, based on
291 pedigree-based relationship.

$$292 \quad Y_i = X_i\beta_i + Z_i\mu_i + e_i$$

293 where Y_i is the binary mortality outcome at the end of the experiment (1 = dead, 2 =
294 alive) of mussel, β_i is the vector of fixed effects, including set of crosses (set 1, set 2),
295 population origins (OLE-PON, WIM, YEU_001), and replication of the experimental
296 infection (EI_1, EI_2 and EI_3). μ_i is the vector of additive genetic effect of the animal,

297 following a normal distribution $\mu \sim N(0, A\sigma_a^2)$, where A is the pedigree relationship
298 matrix, and σ_a^2 is a matrix of additive genetic variance. e_i is the vector of random
299 residuals, assumed to be distributed as $e \sim N(0, I\sigma_e^2)$, where I is an identity matrix and
300 σ_e^2 is a matrix of the residual variance. X_i and Z_i are known incidence matrices relating
301 observations to the fixed and random effects mentioned above.

302 The EBV were estimated using BLUPF90 package and the variance components using
303 AIREMLF90 and THRGIBBS1F90 programs. With the threshold model, the variance
304 components were estimated using a Gibbs sampler with 100,000 iterations, 10,000 of
305 burn-in and one sample was kept every 10 iterations for posterior analysis. Variance
306 components were estimated using the average information restricted maximum
307 likelihood algorithm (Gilmour et al., 1995).

308 Heritability (h^2) was estimated as: $h^2 = \frac{\sigma_a^2}{\sigma_a^2 + \sigma_e^2}$

309 2.7.2 GBLUP

310 The GBLUP model uses the same approach as the PBLUP model, but with μ
311 replaced by g and A replaced by G . Here, g is the vector of additive genomic effects,
312 and G is the genomic relationship matrix. The matrix G was computed as described by
313 VanRaden (2008).

$$314 \quad G = \frac{ZZ'}{\sum_i^m 2p_i(1-p_i)}$$

315 where Z is a matrix of centered genotypes ($0 - 2p =$ homozygous, $1 - 2p =$
316 heterozygous, $2 - 2p =$ homozygous), p_i is the frequency of the reference allele for
317 the i^{th} marker, and m is the total number of markers.

318 Heritability (h^2) was estimated as: $h^2 = \frac{\sigma_g^2}{\sigma_g^2 + \sigma_e^2}$

319 **2.7.3 ssGBLUP**

320 The single-step GBLUP (ssGBLUP) model enhances the PBLUP and GBLUP
321 model by fitting the H matrix, which integrates both genomic and pedigree data (Aguilar
322 et al., 2010). The inverse of the H matrix was constructed as follows:

$$323 \quad H^{-1} = A^{-1} + \begin{bmatrix} 0 & 0 \\ 0 & (0.95G + 0.05A_{22})^{-1} - A_{22}^{-1} \end{bmatrix}$$

324 where G is as described above and A_{22} is the pedigree-based relationship matrix for
325 genotyped animals.

326 Heritability (h^2) was estimated as: $h^2 = \frac{\sigma_h^2}{\sigma_h^2 + \sigma_e^2}$

327

328 **2.8 Genome wide association study**

329 To identify SNPs associated with resistance to *V. splendidus*, a genome wide
330 association study (GWAS) was performed using a mixed linear model association
331 through ssGBLUP analysis. The postGSF90 module (Misztal et al., 2014) from the
332 BLUPF90 package was used to estimate the effects of the SNPs (\hat{a}_i) based on the
333 genomic breeding values \hat{g}_i predicted for the genotyped animals. The SNP effects
334 were estimated according to the following equation:

$$335 \quad \hat{a}_i = dZ'[ZdZ']^{-1}\hat{g}_i$$

336 where d is the vector of weights associated with the SNP effects and Z is the incidence
337 matrix relating SNP effects to genomic breeding values.

338 A linear mixed model was applied to assess resistance to *V. splendidus* on the
339 observed scale, incorporating the genotype of an individual SNP as a fixed effect. The
340 p-values for each SNP were computed using the POSTGSF90 module.

341 For the GWAS, a Bonferroni correction with $\alpha = 5\%$ was used to determine the
342 genome-wide significance threshold $[-\log_{10}(\alpha/n)]$, where $n = 2,204$ (total number of
343 SNPs genome-wide) and the chromosome-wide suggestive threshold $[-\log_{10}(\alpha/m)]$
344 , where $m = 157$ (average number of SNPs per chromosome). Only the SNPs with a
345 $-\log P(\text{value})$ over the chromosome wide threshold were considered to detect QTL
346 associated with the resistance. Genome-wide significant threshold used in this study
347 was considered to $-\log P(\text{value}) = 4.64$, while chromosome-wide significant
348 threshold was opted to $-\log P(\text{value}) = 3.49$.

349 For each QTL, the additive effect (a) of the top SNP was used to estimate the
350 proportion of genetic variance explained by this peak SNP using:

351
$$\%V_g = \frac{2p(1-p)a^2}{\sigma_g^2} * 100$$

352 with σ_g^2 the total genetic variance estimated using the linear mixed model with
353 PROGSF90 and p the minor allele frequency of the target SNP.

354

355 **2.9 Prediction accuracy**

356 Prediction accuracy for the BLUP, GBLUP, and ssGBLUP models was
357 assessed using the 'leave-one-out' method. In this approach, each observation is
358 systematically excluded one at a time. The model is then trained on the remaining data,
359 and the (G)EBV for the excluded individual is predicted by masking its phenotype.

360 The accuracy (r) of prediction was computed as the correlation between the (G)EBVs
361 and the corrected phenotype (\hat{y}) of the mussel divided by the square root of the
362 heritability, using the formula:

$$363 \quad r = \frac{[(G)EBV, \hat{y}]}{\sqrt{h^2}}$$

364 The heritability value (h^2) used in this analysis was calculated using the variance
365 components (σ_a^2 and σ_e^2) from the ssGBLUP model.

366 **2.9.1 Evaluation of the effect of SNP density and training population size on** 367 **genomic predictions**

368 SNP panels of varying densities were assessed by selecting subsets from the
369 full QC-filtered SNP panel for each dataset. Panels of the following densities were
370 tested: 500 SNPs, 1,000 SNPs, 1,500 SNPs, annotated SNPs (~2,200), and all high-
371 quality SNPs (~3,400). SNPs for each panel were selected randomly within each
372 chromosome, with the number of SNPs chosen from each chromosome being
373 proportional to the total number of high-quality SNPs per chromosome. Different
374 training population sizes were evaluated by randomly selecting subsets from the
375 population. Training population of 100, 300, 500, and all individuals were tested using
376 annotated SNPs panel information. The analysis performed only with the ssGBLUP
377 model, which is known for its effectiveness in genomic selection. To mitigate biases,
378 we generated five different SNP panels for each SNP density randomly, and similarly
379 five subsets randomly selected for each training population to address size-based
380 selection biases.

381

382 **3. Results**

383 **3.1 *Vibrio* challenge**

384 The cumulative mortality rate 72 hours post-injection was 47%. At endpoint,
385 mortality rates were 63% for EI_1, 41% for EI_2, and 37% for EI_3. Among mussel
386 populations, the WIM population (54%) showed higher susceptibility to *V. splendidus*
387 compared to the YEU_001 (45%) and OLE-PON (37%) populations. Mortality rates
388 varied significantly among families upon exposure to *V. splendidus*, ranging from 17%
389 to 83%. The mean mortality rates for all families are depicted in Figure 1.

390

391 **3.2 Population structure**

392 Figure 2 illustrates the results of the principal component analysis (PCA),
393 revealing the population structure of the mussel population. The first two PCA axes
394 collectively account for over 15% of the total genetic variation. The populations were
395 generally homogeneous, with the exception of two families whose offspring showed
396 greater isolation from others. F_{ST} analysis revealed low genetic differentiation between
397 populations. The mean genetic distances between populations are shown in Table 2,
398 with F_{ST} values ranging from 0.02 to 0.03, suggesting genetic similarity across all three
399 populations (Figure 3). Overall, the absence of significant genetic differentiation
400 between populations provides favorable conditions to merge data from all the
401 populations for performing genomic selection analysis.

402

403 **3.3 SNP mapping and genome coverage**

404 In fact, 2,204 SNPs were positioned on the reference genome, resulting a loss
405 of 1,202 SNPs. The positions of markers on the chromosomes is illustrated in Figure

406 4. The average SNP density per megabase (Mb) ranges from 0.57 to 2.37, varying
407 among chromosomes and within chromosome (Supplementary Table 2).
408 Approximately, only 9% of all 1 Mb segments contain more than 5 SNPs. SNP density
409 exhibits non-uniformity throughout the genome, with each chromosome demonstrating
410 varying densities. The lower marker density results in greater mean average distances
411 between adjacent SNPs, ranged from 421 kb to 1739 kb depending on the
412 chromosome.

413

414 **3.4 Linkage disequilibrium analysis**

415 Figure 5 illustrates that linkage disequilibrium (LD) decreases sharply as the
416 distance between pairs of SNPs increases, with the most rapid decline occurring within
417 the first 100 kb. Beyond this range, LD continues to decline and becomes more
418 variable. The OLE-PON population consistently shows higher LD throughout the
419 genome compared to other populations. On average, the LD values (r^2) for SNPs less
420 than 15 kb apart are 0.12 for OLE-PON, 0.10 for WIM, and 0.06 for YEU. Linkage
421 disequilibrium values are generally low between adjacent SNPs for all the
422 chromosomes, where distances between adjacent SNPs are larger.

423

424 **3.5 Heritability**

425 The estimates of heritability using the linear and Gibbs sampling models are
426 summarized in Table 3. Pedigree-based heritability estimates for resistance to *V.*
427 *splendidus* in *M. edulis* ranged from 0.22 to 0.31. Genomic heritability was slightly
428 higher, varying between 0.33 and 0.36. The ssGBLUP based estimated heritability
429 ranging from 0.28 to 0.33, which combines genomic and pedigree information

430

431 **3.6 Genetic architecture**

432 GWAS for resistance to *V. splendidus* identified only one significant SNP
433 surpassing the genome-wide threshold on chr 2, and seven significant SNPs
434 surpassing the suggestive chromosome-wide threshold on chr 2, chr 4, chr 7, chr 9,
435 chr 12, and chr 13 (Figure 6 and Table 4). However, none of these markers explained
436 more than 1.06% of genetic variance (Figure 7 and Table 4).

437

438 **3.7 Prediction accuracy**

439 Accuracy with all data are 0.36, 0.43, 0.43 for BLUP, GBLUP and ssGBLUP,
440 respectively. Genomic selection (GBLUP and ssGBLUP) is better than BLUP by 19%.
441 Overall, prediction accuracy for GS increased with the density of markers (Figure 8).
442 Incorporating genomic information generally enhanced accuracy compared to
443 pedigree-based estimation, except with 500 SNPs where PBLUP exhibited higher
444 accuracy than GBLUP (Figure 8). With maximum training population and SNP subsets,
445 genomic evaluation improved accuracy by 17%, 19%, 25%, and 19% for 1,000, 1,500,
446 annotated (2,204), and all SNPs (3,400), respectively, compared to PBLUP. When
447 comparing GBLUP and ssGBLUP models, the prediction accuracy was consistently
448 favored the ssGBLUP model, except when using annotated SNPs in the GBLUP model
449 (Figure 8). In evaluating the size of the training population, accuracy ranged from 0.50
450 to 0.36 in BLUP, and from 0.47 to 0.45 in ssGBLUP with sizes from 100 to all
451 individuals, respectively (Figure 9).

452

453 **4. Discussion**

454 In our study, we aimed to demonstrate the feasibility of genomic selection in a
455 mussel breeding program in France. We used a recently developed multi species
456 medium-density 60K SNP-array (Nascimento-Schulze et al., 2023) to perform genomic
457 analysis.

458

459 **4.1 Genotyping quality and genome covering by selected SNPs**

460 To the best of our knowledge, our study is the first to use the multi species
461 medium-density 60K SNP-array (Nascimento-Schulze et al., 2023) to estimate genetic
462 parameters in blue mussel (*M. edulis*). Following the AxAS software's best-practice
463 workflow with minor adjustments to thresholds, we identified 7,476 poly high-quality
464 SNPs from 23,252 initially screened SNPs across 768 individuals. The necessity for
465 stringent filtering of genotyping data is highlighted by the prevalence of poor-quality
466 markers. After quality control using plink, we retained 3,406 SNPs, representing only
467 15% of the total SNPs designed for *M. edulis*. This reduction may be attributed to the
468 polymorphic nature of mussel species or limited number of individuals used to
469 construct the SNP array design (Gerdol et al., 2020; Nascimento-Schulze et al., 2023).

470 The *Mytilus* genus exhibits a complex evolutionary history characterized by
471 extensive gene flow among congeneric species, and its genome is known for its
472 complexity and high degree of polymorphism (Gerdol et al., 2020; Smietanka et al.,
473 2014). The array used in the present study was developed using a whole-genome low
474 coverage approach. Out of 23,253 poly high SNPs identified in *M. edulis*, only 16,213
475 (70%) were annotated on the recently published reference genome of *M. edulis*.
476 Assembly errors in the reference genome may rise from several factors, such as

477 exceptionally high genetic polymorphism levels, non-Mendelian segregation of marker
478 loci in paired crosses, and a significant occurrence of null alleles in genetic markers
479 (Hedgecock et al., 2015). While a moderate proportion of our selected markers (3,406
480 out of 23,252) aligned well with the latest reference genome (2,204 SNPs; 65%), we
481 observed a sparse distribution of SNPs across the linkage map. This limited coverage
482 and sparse SNP distribution could potentially lead to the omission of QTLs in specific
483 regions, suggesting the necessity for developing an optimized SNP array to address
484 these challenges effectively. The bi-species Axiom Affymetrix 57K SNP array has been
485 used in Pacific oysters, where applying the AxAS software's best practice workflow led
486 to a notable reduction in the number of informative SNPs. Specifically, Gutierrez et al.
487 (2018) reported 23,000 informative SNPs from 820 individuals, Vendrami et al. (2019)
488 identified 21,499 SNPs from 232 individuals, and Jourdan et al. (2023) obtained 14,500
489 SNPs from 2,420 individuals. This reduction is largely attributed to the complex genetic
490 structure of molluscs, stemming from the highly polymorphic nature of their genomes
491 (Jiao et al., 2021; Song et al., 2021), and is further influenced by the genetic
492 relationship between the training population used for array design and the breeding
493 candidates in selective program (Houston et al., 2020). However, recent studies on
494 bivalves have demonstrated that a moderate number of high-quality markers (1,000 -
495 3,000) could suffice for accurate predictions (Gutierrez et al., 2018; Kriaridou et al.,
496 2020; Penaloza et al., 2022).

497

498 **4.2 Linkage disequilibrium**

499 Linkage disequilibrium (LD) at the genome level plays a crucial role in the
500 efficacy of breeding programs, influencing genetic variance and the accuracy of

501 association analyses (Goddard and Hayes, 2009; Siol et al., 2017). In our study, values
502 for r^2 ranged between 0.07 and 0.09 for SNPs within a distance of 10 kb and from 0.03
503 to 0.08 within 50 kb across the studied populations. However, LD levels decreased to
504 less than 0.05 at 100 kb in two populations. Overall, LD between adjacent markers
505 within each population was predominantly less than 0.1 within 2 kb, indicating a rapid
506 decline in LD within the blue mussel genome. This swift decay suggests a historically
507 large effective population size and high recombination rate, reflecting substantial
508 genetic diversity within the population (Ellegren and Galtier, 2016). Moreover, LD
509 values are population-specific, and influenced by evolutionary factors such as natural
510 selection, mutation, genetic drift, line origin and migration, as well as molecular forces
511 including historical recombination events, and breeding history such as historical
512 effective population sizes, intensity and direction of artificial selection, population
513 admixture, and mating patterns (Du et al., 2007). Our findings confirm the low LD in *M.*
514 *edulis* populations, consistent with previous studies on bivalves (Jones et al., 2013b;
515 Jourdan et al., 2023; Vera et al., 2022).

516

517 **4.3 Population structure**

518 F_{ST} is widely applied to evaluate genetic differentiation between/among
519 populations (Hu et al., 2022). The low F_{ST} values ($F_{ST} < 0.03$) observed in our study
520 suggest minimal genetic differentiation among mussel populations, indicating a lack of
521 significant genetic structure. This phenomenon may be attributed to similar selection
522 pressure and limited gene flow among the mussel populations, irrespective of
523 geographic location. Similar findings have been reported in other studies, such as
524 pairwise F_{ST} (< 0.02) among wild edible cockle using SNPs information (Vera et al.,

525 2022) and among wild populations of Pacific oyster using allozymes and microsatellites
526 markers (Appleyard and Ward, 2006).

527 PCA provided robust evidence supporting the classification of mussels into the
528 same groups, consistent with the low F_{ST} values observed. The PCA did not reveal
529 population genetic stratification except in two families in WIM population, suggesting
530 that the observed genetic variation is homogeneous and indicative of genetic proximity
531 among populations. The two families whose offspring showed greater isolation from
532 others in the WIM population may be due to due to the peculiar characteristics of the
533 parents, which drive the first axis of the PCA.

534

535 **4.4 Heritability**

536 Our study presents the first report of heritability estimates for resistance to *V.*
537 *splendidus* experimental infection in *M. edulis* based on genome-wide SNPs. We
538 observed moderate heritability for *V. splendidus* resistance (0.22–0.36), which are
539 higher compared to our previous study using the same population. This increase may
540 be attributed to the inclusion of a third experimental infection in this study, despite the
541 overall lower mortality rate (Ajithkumar et al., 2024b). Disease resistance to pathogens
542 in bivalves seems to be a heritable trait, with moderate to high heritability in oysters,
543 clams, and abalone, ranging from 0.21 to 0.63 (Brokordt et al., 2017; Dégremonet et al.,
544 2015; Smits et al., 2020). Studies on oysters have shown varying levels of heritability
545 (h^2 : 0.09-0.54) against different *Vibrio spp.* pathogens at different life stages (Azema
546 et al., 2017; Dietrich et al., 2022; Nordio et al., 2021; Zhai et al., 2021). Comparing
547 heritability estimates among methods, both GBLUP and ssGBLUP consistently
548 showed higher heritability compared to pedigree-based methods. This difference is

549 likely due to the genomic relationship matrix constructed based on genome-wide SNPs
550 information can capture both within and between-family genetic variance, whereas
551 traditional pedigree selection only captures genetic variance between families (Boudry
552 et al., 2021). To date, numerous studies across aquaculture species have similarly
553 demonstrated that GBLUP methods provide higher estimated heritability and greater
554 accuracy compared to PBLUP (Gutierrez et al., 2018; Tsai et al., 2015). These results
555 underscore the presence of genetic variation for resistance to *V. splendidus* in our
556 mussel populations, and highlight significant opportunities for enhancing disease
557 resistance through selective breeding programs, whether using pedigree-based or
558 genomic selection strategies.

559

560 **4.5 Genome wide association study**

561 QTL detection in our populations posed challenges due to limited number of
562 markers and individuals. Given the data in the current study do suggest a polygenic
563 nature of resistance to *V. splendidus*, utilizing all markers to calculate genomic
564 breeding values for resistance may be the most effective approach. Our association
565 analyses suggest that resistance against *V. splendidus* exhibits a polygenic
566 architecture without major QTLs. Similar findings have been reported for bacterial
567 disease resistance in various aquaculture species including, Atlantic salmon (Correa
568 et al., 2015), Coho salmon (Barría et al., 2018), Gilthead Sea Bream (Palaikostas et
569 al., 2016), European seabass (Oikonomou et al., 2022), and Pacific Oyster (Yang et
570 al., 2022). For instance, a study on catfish identified four QTLs associated with
571 columnaris resistance using a high-density SNP array (Geng et al., 2015), highlighting
572 the importance of high-density SNP array for GWAS studies. Our study used 2,204
573 SNPs, which may not provide sufficient coverage given the rapid LD decay, potentially

574 leading to the omission of important QTLs. This underscores the need for increased
575 SNP coverage to ensure robust association analyses (Jones et al., 2013b).
576 Additionally, a larger number of individuals (> 1,000) would be beneficial for enhancing
577 overall QTL detection (Barría et al., 2018). Future studies could benefit from using a
578 greater number of markers and phenotypes, as well as by creating resistant and
579 susceptible lines in the F2 generation. These approaches can exploit more genetic
580 variation and assist in identifying potential QTLs (Geng et al., 2015).

581

582 **4.6 Prediction accuracy**

583 The accuracy of genomic selection is affected by several factors, including the
584 relationship between training and validation animals, sample size in the reference
585 population, marker density, effective population size, LD structure, underlying trait
586 architecture and heritability of trait (Yáñez et al., 2023). Therefore, the lower range of
587 the prediction accuracies estimated here may reflect the underlying trait architecture
588 or marker density. The choice of genomic selection model for breeding programs
589 requires a prior understanding of the genetic architecture of the selected trait(s). In the
590 current study on *M. edulis* populations, the genetic contribution to the observed
591 variation in resistance to *V. splendidus* was largely polygenic in nature. For the
592 improvement of polygenic traits, GBLUP is the most reliable model and typically
593 provides the highest prediction accuracy for highly polygenic traits, while the Bayesian
594 models are preferable for traits controlled by few large effect loci in genomic selection
595 (Legarra et al., 2015; Yáñez et al., 2023)

596 Genomic selection improves accuracy of up to 19% compared to pedigree
597 selection. A key consideration for the commercial implementation of genomic selection

598 in shellfish aquaculture is the high cost of genotyping. Reference population size and
599 marker density are two key factors for effectively reducing the cost of genomic selection
600 (Song et al., 2022). Applying a low density SNP panel is one way to increase economic
601 viability of genomic selection (Kriaridou et al., 2020). The prediction accuracies for
602 genomic models in our study ranged from 0.32 to 0.48 for resistance to *V. splendidus*
603 (with SNP densities ranging from 500 to ~3400), whereas the accuracy of PBLUP was
604 0.36. This result is slightly lower than the ranges reported for disease-related traits in
605 other bivalve species. For instance, genomic selection prediction accuracies from
606 GBLUP models for resistance to Ostreid herpesvirus (OsHV-1-Ivar) ranged from 0.68
607 to 0.76 in the Pacific oyster (Gutierrez et al., 2020). Prediction accuracies for growth-
608 related traits using the GBLUP model in other bivalves are relatively similar, e.g., 0.52-
609 0.73 in the Pacific oyster (Gutierrez et al., 2018; Jourdan et al., 2023), 0.67-0.79 in the
610 Portuguese oyster (Vu et al., 2021), and > 0.83 in European flat oyster (Penaloza et
611 al., 2022). Other reports on genomic prediction accuracies for disease-related traits in
612 finfish aquaculture species show the prediction accuracies as low as 0.21, reviewed in
613 Houston et al. (2020) and 0.25 - 0.48 for growth related-traits in the Zhikong scallop
614 (Wang et al., 2018). However, this result highlight that genomic selection is a useful
615 approach to increase resistance to *V. splendidus* in our blue mussel populations.

616 Overall, our results showed that genomic methods predict better accuracy (25 -
617 33%) for resistance to *V. splendidus* using ~2000 SNPs in a family-based design
618 compared to pedigree-based estimation. This indicates that substantial improvements
619 in the rate of genetic gain can be achieved through genomics-based selection
620 techniques. It also increases the possibility of a low-density genomic selection
621 approach for *Vibrio* resistance in mussel breeding, as low-density genotyping can be
622 substantially cheaper than high-density SNP arrays. Furthermore, studies on disease

623 resistance in the Pacific oyster, growth traits in the European flat oyster, and heat
624 tolerance in the Pacific abalone have shown that low-density SNP panels of around
625 1000-2000 SNPs can achieve EBV accuracies similar to those obtained with medium-
626 density arrays (Gutierrez et al., 2020; Kriaridou et al., 2020; Liu et al., 2022; Penalosa
627 et al., 2022). Similar findings in multiple aquatic species have shown that low-density
628 panels can achieve higher accuracies than the pedigree-based approach, making
629 them a feasible alternative for identifying candidates with the highest genetic merit for
630 complex traits such as growth and disease resistance (Kriaridou et al., 2020).

631 Although the mussel genome is 1.4 Gb in size, our study suggests that a
632 relatively low number of genetic markers can still achieve high prediction accuracy,
633 with a rapid LD decay observed across all populations. Additionally, both the training
634 and validation datasets comprised closely related animals (half-sibs/full-sibs). These
635 individuals will share large genomic segments, which can be captured by few markers.
636 However, as the genetic distance between the training and validation sets increases,
637 genomic prediction accuracy is likely to decrease (Palaiokostas et al., 2019).
638 Therefore, regular mating among close relatives of breeding candidates is required to
639 maintain prediction accuracy (Gutierrez et al., 2020). Moreover, additional populations
640 with different effective population sizes, genetic backgrounds, and degrees of
641 relatedness should be assessed to obtain estimates expected in practical breeding
642 programs.

643 Although our results highlight the possibility of reducing the genotyping costs
644 associated with genomic prediction approaches, caution should be exercised
645 regarding the smallest marker density. Our study found that using only 500 SNPs in
646 the GBLUP model resulted in an estimated decrease in the accuracy of genomic
647 breeding values (GEBVs) for resistance to *V. splendidus* by 11% compared to PBLUP.

648 It's important to note that when both pedigree information and genotypes are available,
649 using ssGBLUP is preferable, as it demonstrates superior accuracy compared to
650 PBLUP. Furthermore, our findings emphasize that annotated SNPs on the *M. edulis*
651 genome provided more information about the studied population and led to higher
652 prediction accuracy than using all SNPs in either the GBLUP or ssGBLUP model. This
653 difference could be due to even distribution of phenotypes among genotyped
654 individuals (50% mortality), or unannotated markers may introduce noise, thereby
655 affecting the accuracy of GEBV estimation. Further investigations using more SNPs,
656 and larger reference population hold potential for genomic selection to further increase
657 the prediction accuracy for host resistance to *V. splendidus* in farmed mussel
658 populations.

659

660 **5. Conclusions**

661 Our study estimated moderate heritability for resistance to *V. splendidus* in blue
662 mussel populations using both pedigree and genomic data from a challenge
663 experiment. GWAS analysis suggests that the trait is polygenic, indicating that
664 genomic selection is more effective than marker-assisted selection. We found that
665 genomic selection can improve accuracy by up to 19% compared to pedigree-based
666 selection. Additionally, our results show the potential for reducing the number of
667 markers, which could make genomic selection more cost-effective. Overall, selective
668 breeding appears to be a promising approach to enhance resistance to *V. splendidus*
669 in blue mussels, and genomic selection could significantly increase genetic gains.

670

671 **Funding**

672 This work was supported by DPAM of the French Ministries of Ecology and Agriculture
673 through the research program “MORBLEU” and the European Union's Horizon 2020
674 research and innovation programme under the Marie Skłodowska-Curie grant
675 agreement No 956697.

676

677 **Author contributions**

678 Munusamy Ajithkumar: Data curation, Formal analysis, Software, Visualization, Writing
679 - original draft, and Writing - review & editing. Jonathan D'Ambrosio: Software, Writing
680 - review & editing. Marie-Agnès Travers: Methodology, Writing - review & editing.
681 Romain Morvezen: Supervision, Software, Writing - review & editing. Lionel
682 Dégremon: Conceptualization, Funding acquisition, Methodology, Supervision;
683 Writing - review & editing.

684

685 **Declaration of Competing Interest**

686 The authors declare that they have no known competing financial interests or personal
687 relationships that could have appeared to influence the work reported in this paper.

688

689 **Data availability**

690 Data will be made available upon reasonable request

691

692 **Acknowledgements**

693 We would like to thank René Robert from LERPC-Ifremer and his colleagues for
694 sampling mussel populations, Hatchery and nursery teams for their help to grow and
695 protect the mussels inside the secured facilities, Delphine Tourbiez for her assistance
696 to experimental infection. We express our sincere thanks to Vincent Paillet for helping
697 to annotate the SNPs on the reference genome.

698

699

700 References

- 701 Aguilar, I., Misztal, I., Johnson, D.L., Legarra, A., Tsuruta, S., Lawlor, T.J., 2010. Hot topic: A unified
702 approach to utilize phenotypic, full pedigree, and genomic information for genetic evaluation of
703 Holstein final score. *J Dairy Sci* 93(2), 743-752. <https://doi.org/10.3168/jds.2009-2730>
- 704 Ajasa, A.A., Boison, S.A., Gjoen, H.M., Lillehammer, M., 2024. Accuracy of genomic prediction using
705 multiple Atlantic salmon populations. *Genet Sel Evol* 56(1). <https://doi.org/10.1186/s12711-024-00907-5>
- 706 Ajithkumar, M., Dégremont, L., Garcia, C., Ledu, C., Benabdelmouna, A., 2024a. Divergent selection for
707 cytogenetic quality in mussel species. Preprint.
- 708 Ajithkumar, M., Lillehammer, M., Travers, M.-A., Maurouard, E., Aslam, M.L., Dégremont, L., 2024b.
709 Genetic parameters for resistance to field mortality outbreaks and resistance to a pathogenic strain of
710 *Vibrio splendidus* in *Mytilus edulis*, *Mytilus galloprovincialis* and natural hybrid. *Aquaculture* 590(0044-
711 8486). <https://doi.org/https://doi.org/10.1016/j.aquaculture.2024.741034>
- 712 Alcapán, A.C., Nespolo, R.F., Toro, J.E., 2007. Heritability of body size in the Chilean blue mussel
713 (*Mytilus chilensis* Hupe´ 1854): effects of environment and ageing. *Aquac Res* 38(3), 313-320.
714 <https://doi.org/10.1111/j.1365-2109.2007.01678.x>
- 715 Allam, B., Raftos, D., 2015. Immune responses to infectious diseases in bivalves. *J Invertebr Pathol* 131,
716 121-136. <https://doi.org/10.1016/j.jip.2015.05.005>
- 717 Appleyard, S.A., Ward, R.D., 2006. Genetic diversity and effective population size in mass selection
718 lines of Pacific oyster (*Crassostrea gigas*). *Aquaculture* 254(1-4), 148-159.
719 <https://doi.org/10.1016/j.aquaculture.2005.10.017>
- 720 Avdelas, L., Avdic-Mravljje, E., Marques, A.C.B., Cano, S., Capelle, J.J., Carvalho, N., Cozzolino, M.,
721 Dennis, J., Ellis, T., Polanco, J.M.F., Guillen, J., Lasner, T., Le Bihan, V., Llorente, I., Mol, A., Nicheva, S.,
722 Nielsen, R., van Oostenbrugge, H., Villasante, S., Visnic, S., Zhelev, K., Asche, F., 2021. The decline of
723 mussel aquaculture in the European Union: causes, economic impacts and opportunities. *Rev Aquacult*
724 13(1), 91-118. <https://doi.org/10.1111/raq.12465>
- 725 Azema, P., Lamy, J.B., Boudry, P., Renault, T., Travers, M.A., Degremont, L., 2017. Genetic parameters
726 of resistance to *Vibrio aestuarianus*, and OsHV-1 infections in the Pacific oyster, *Crassostrea gigas*, at
727 three different life stages. *Genet Sel Evol* 49. <https://doi.org/10.1186/s12711-017-0297-2>
- 728 Bai, Z.Y., Li, Q.Q., Han, X.K., Li, J.L., 2017. Estimates of genetic parameters and genotype by
729 environment interactions for shell nacre color and growth traits in the purple freshwater pearl mussel
730 *Hyriopsis cumingii*. *Aquacult Int* 25(6), 2079-2090. <https://doi.org/10.1007/s10499-017-0170-x>
- 731 Barría, A., Christensen, K.A., Yoshida, G.M., Correa, K., Jedlicki, A., Lhorente, J.P., Davidson, W.S., Yáñez,
732 J.M., 2018. Genomic Predictions and Genome-Wide Association Study of Resistance Against
733

734 Piscirickettsia salmonis in Coho Salmon (*Oncorhynchus kisutch*) Using ddRAD Sequencing. *G3-Genes*
735 *Genomes Genetics* 8(4), 1183-1194. <https://doi.org/10.1534/g3.118.200053>

736 Bechemin, C., Soletchnik, P., Polsenaere, P., Le Moine, O., Pernet, F., Protat, M., Fuhrmann, M., Quere,
737 C., Goulitquer, S., Corporeau, C., Lapegue, S., Travers, M.-A., Morga, B., Garrigues, M., Garcia, C.,
738 Haffner, P., Dubreuil, C., Faury, N., Baillon, L., Baud, J.-P., Renault, T., 2015. Episodes de mortalité
739 massive de moules bleues observés en 2014 dans les Pertuis charentais. *Bulletin Epidémiologie, Santé*
740 *animale et alimentation*. (67). 6-9.

741 Ben Cheikh, Y., Travers, M.A., Le Foll, F., 2017. Infection dynamics of a *V. splendidus* strain pathogenic
742 to *Mytilus edulis*: In vivo and in vitro interactions with hemocytes. *Fish Shellfish Immun* 70, 515-523.
743 <https://doi.org/10.1016/j.fsi.2017.09.047>

744 Ben Cheikh, Y., Travers, M.A., Morga, B., Godfrin, Y., Le Foll, F., 2016. First evidence for a *Vibrio* strain
745 pathogenic to *Mytilus edulis* altering hemocyte immune capacities. *Fish Shellfish Immun* 53, 91-91.

746 Bódis, E., Tóth, B., Sousa, R., 2014. Massive mortality of invasive bivalves as a potential resource
747 subsidy for the adjacent terrestrial food web. *Hydrobiologia* 735(1), 253-262.
748 <https://doi.org/10.1007/s10750-013-1445-5>

749 Boudry, P., Allal, F., Aslam, M.L., Bargelloni, L., Bean, T.P., Brard-Fudulea, S., Briec, M.S.O., Calboli,
750 F.C.F., Gilbey, J., Haffray, P., Lamy, J.B., Morvezen, R., Purcell, C., Prodohl, P.A., Vandeputte, M.,
751 Waldbieser, G.C., Sonesson, A.K., Houston, R.D., 2021. Current status and potential of genomic
752 selection to improve selective breeding in the main aquaculture species of International Council for
753 the Exploration of the Sea (ICES) member countries. *Aquaculture Reports* 20.
754 <https://doi.org/10.1016/j.aqrep.2021.100700>

755 Brokordt, K., González, R., Fariás, W., Winkler, F.E., Lohrmann, K.B., 2017. First insight into the heritable
756 variation of the resistance to infection with the bacteria causing the withering syndrome disease in
757 *Haliotis rufescens* abalone. *J Invertebr Pathol* 150, 15-20. <https://doi.org/10.1016/j.jip.2017.08.014>

758 Camara, M.D., Symonds, J.E., 2014. Genetic improvement of New Zealand aquaculture species:
759 programmes, progress and prospects. *New Zeal J Mar Fresh* 48(3), 466-491.
760 <https://doi.org/10.1080/00288330.2014.932291>

761 Capelle, J.J., Garcia, A.B., Kamermans, P., Engelsma, M.Y., Jansen, H.M., 2021. Observations on recent
762 mass mortality events of marine mussels in the Oosterschelde, the Netherlands. *Aquacult Int* 29(4),
763 1737-1751. <https://doi.org/10.1007/s10499-021-00713-6>

764 Chang, C.C., Chow, C.C., Tellier, L.C.A.M., Vattikuti, S., Purcell, S.M., Lee, J.J., 2015. Second-generation
765 PLINK: rising to the challenge of larger and richer datasets. *Gigascience* 4.
766 <https://doi.org/10.1186/s13742-015-0047-8>

767 Charles, M., Bernard, I., Villalba, A., Oden, E., Burioli, E.A.V., Allain, G., Trancart, S., Bouchart, V.,
768 Houssin, M., 2020a. High mortality of mussels in northern Brittany - Evaluation of the involvement of
769 pathogens, pathological conditions and pollutants. *J Invertebr Pathol* 170.
770 <https://doi.org/10.1016/j.jip.2019.107308>

771 Charles, M., Trancart, S., Oden, E., Houssin, M., 2020b. Experimental infection of by two -related
772 strains: Determination of pathogenicity level of strains and influence of the origin and annual cycle of
773 mussels on their sensitivity. *J Fish Dis* 43(1), 9-21. <https://doi.org/10.1111/jfd.13094>

774 Correa, K., Bangerla, R., Figueroa, R., Lhorente, J.P., Yáñez, J.M., 2017. The use of genomic information
775 increases the accuracy of breeding value predictions for sea louse (*Caligus rogercresseyi*) resistance in
776 Atlantic salmon (*Salmo salar*). *Genet Sel Evol* 49. <https://doi.org/10.1186/s12711-017-0291-8>

777 Correa, K., Lhorente, J.P., López, M.E., Bassini, L., Naswa, S., Deeb, N., Di Genova, A., Maass, A.,
778 Davidson, W.S., Yáñez, J.M., 2015. Genome-wide association analysis reveals loci associated with
779 resistance against *Piscirickettsia salmonis* in two Atlantic salmon (*Salmo salar* L.) chromosomes. *Bmc*
780 *Genomics* 16. <https://doi.org/10.1186/s12864-015-2038-7>

781 D'Ambrosio, J., Phocas, F., Haffray, P., Bestin, A., Brard-Fudulea, S., Poncet, C., Quillet, E., Dechamp,
782 N., Fraslín, C., Charles, M., Dupont-Nivet, M., 2019. Genome-wide estimates of genetic diversity,
783 inbreeding and effective size of experimental and commercial rainbow trout lines undergoing selective
784 breeding. *Genet Sel Evol* 51. <https://doi.org/10.1186/s12711-019-0468-4>

785 Dégremont, L., Garcia, C., Allen, S.K., 2015. Genetic improvement for disease resistance in oysters: A
786 review. *J Invertebr Pathol* 131, 226-241. <https://doi.org/10.1016/j.jip.2015.05.010>

787 Dégremont, L., Maurouard, E., Rabiller, M., Glize, P., 2019. Response to selection for increasing
788 resistance to the spring mortality outbreaks in *Mytilus edulis* occurring in France since 2014.
789 *Aquaculture* 511. <https://doi.org/10.1016/j.aquaculture.2019.734269>

790 Díaz-Puente, B., Guiñez, R., Pita, A., Miñambres, M., Presa, P., 2020. Genotype by environment
791 interaction for shell length in *Mytilus galloprovincialis*. *J Exp Mar Biol Ecol* 522.
792 <https://doi.org/10.1016/j.jembe.2019.151252>

793 Dietrich, J.P., Hicks, M.B.R., Hard, J.J., Nichols, K.M., Langdon, C.J., Divilov, K., Schoolfield, B., Arkoosh,
794 M.R., 2022. Heritability estimates of disease resistance to *Vibrio coralliitcticus* in Pacific oyster
795 (*Crassostrea gigas*) larvae from a selective broodstock program. *Aquaculture* 560.
796 <https://doi.org/10.1016/j.aquaculture.2022.738492>

797 Du, F.X., Clutter, A.C., Lohuis, M.M., 2007. Characterizing linkage disequilibrium in pig populations. *Int*
798 *J Biol Sci* 3(3), 166-178.

799 Ellegren, H., Galtier, N., 2016. Determinants of genetic diversity. *Nat Rev Genet* 17(7), 422-433.
800 <https://doi.org/10.1038/nrg.2016.58>

801 Ericson, J.A., Venter, L., Copedo, J.S., Nguyen, V.T., Alfaro, A.C., Ragg, N.L.C., 2023. Chronic heat stress
802 as a predisposing factor in summer mortality of mussels, *Perna canaliculus*. *Aquaculture* 564.
803 <https://doi.org/10.1016/j.aquaculture.2022.738986>

804 FAO, 2023. The State of World Fisheries and Aquaculture 2022. Fishstat Plus.

805 Geng, X., Sha, J., Liu, S.K., Bao, L.S., Zhang, J.R., Wang, R.J., Yao, J., Li, C., Feng, J.B., Sun, F.Y., Sun, L.Y.,
806 Jiang, C., Zhang, Y., Chen, A.L., Dunham, R., Zhi, D.G., Liu, Z.J., 2015. A genome-wide association study
807 in catfish reveals the presence of functional hubs of related genes within QTLs for columnaris disease
808 resistance. *Bmc Genomics* 16. <https://doi.org/10.1186/s12864-015-1409-4>

809 Gerdol, M., Moreira, R., Cruz, F., Gomez-Garrido, J., Vlasova, A., Rosani, U., Venier, P., Naranjo-Ortiz,
810 M.A., Murgarella, M., Greco, S., Balseiro, P., Corvelo, A., Frias, L., Gut, M., Gabaldon, T., Pallavicini, A.,
811 Canchaya, C., Novoa, B., Alioto, T.S., Posada, D., Figueras, A., 2020. Massive gene presence-absence
812 variation shapes an open pan-genome in the Mediterranean mussel. *Genome Biol* 21(1).
813 <https://doi.org/10.1186/s13059-020-02180-3>

814 Gilmour, A.R., Thompson, R., Cullis, B.R., 1995. Average information REML: An efficient algorithm for
815 variance parameter estimation in linear mixed models. *Biometrics* 51(4), 1440-1450.
816 <https://doi.org/10.2307/2533274>

817 Gjedrem, T., Rye, M., 2018. Selection response in fish and shellfish: a review. *Rev Aquacult* 10(1), 168-
818 179. <https://doi.org/10.1111/raq.12154>

819 Goddard, M.E., Hayes, B.J., 2009. Mapping genes for complex traits in domestic animals and their use
820 in breeding programmes. *Nat Rev Genet* 10(6), 381-391. <https://doi.org/10.1038/nrg2575>

821 Griot, R., Allal, F., Brard-Fudulea, S., Morvezen, R., Haffray, P., Phocas, F., Vandeputte, M., 2020. APIS:
822 An auto-adaptive parentage inference software that tolerates missing parents. *Mol Ecol Resour* 20(2),
823 579-590. <https://doi.org/10.1111/1755-0998.13103>

824 Guiñez, R., Toro, J.E., Krapivka, S., Alcapán, A.C., Oyarzún, P.A., 2017. Heritabilities and genetic
825 correlation of shell thickness and shell length growth in a mussel, *Mytilus chilensis* (Bivalvia:Mytilidae).
826 *Aquac Res* 48(4), 1450-1457. <https://doi.org/10.1111/are.12981>

827 Guo, X.M., Puritz, J.B., Wang, Z.W., Proestou, D., Allen, S., Small, J., Verbyla, K., Zhao, H.G., Haggard, J.,
828 Chriss, N., Zeng, D., Lundgren, K., Allam, B., Bushek, D., Gomez-Chiarri, M., Hare, M., Hollenbeck, C., La
829 Peyre, J., Liu, M., Lotterhos, K.E., Plough, L., Rawson, P., Rikard, S., Saillant, E., Varney, R., Wikfors, G.,
830 Wilbur, A., 2023. Development and Evaluation of High-Density SNP Arrays for the Eastern Oyster. *Mar*
831 *Biotechnol* 25(1), 174-191. <https://doi.org/10.1007/s10126-022-10191-3>

832 Gutierrez, A.P., Matika, O., Bean, T.P., Houston, R.D., 2018. Genomic Selection for Growth Traits in
833 Pacific Oyster (*Crassostrea gigas*): Potential of Low-Density Marker Panels for Breeding Value
834 Prediction. *Front Genet* 9. <https://doi.org/10.3389/fgene.2018.00391>

835 Gutierrez, A.P., Symonds, J., King, N., Steiner, K., Bean, T.P., Houston, R.D., 2020. Potential of genomic
836 selection for improvement of resistance to ostreid herpesvirus in Pacific oyster (*Crassostrea gigas*).
837 *Anim Genet* 51(2), 249-257. <https://doi.org/10.1111/age.12909>
838 Gutierrez, A.P., Turner, F., Gharbi, K., Talbot, R., Lowe, N.R., Peñaloza, C., McCullough, M., Prodöhl,
839 P.A., Bean, T.P., Houston, R.D., 2017. Development of a Medium Density Combined-Species SNP Array
840 for Pacific and European Oysters (*Crassostrea gigas* and *Ostrea edulis*). *G3-Genes Genomes Genetics*
841 7(7), 2209-2218. <https://doi.org/10.1534/g3.117.041780>
842 Hedgecock, D., Shin, G., Gracey, A.Y., Van Den Berg, D., Samanta, M.P., 2015. Second-Generation
843 Linkage Maps for the Pacific Oyster *Crassostrea gigas* Reveal Errors in Assembly of Genome Scaffolds.
844 *G3-Genes Genomes Genetics* 5(10), 2007-2019. <https://doi.org/10.1534/g3.115.019570>
845 Hollenbeck, C.M., Johnston, I.A., 2018. Genomic Tools and Selective Breeding in Molluscs. *Front Genet*
846 9. <https://doi.org/10.3389/fgene.2018.00253>
847 Houston, R.D., Bean, T.P., Macqueen, D.J., Gundappa, M.K., Jin, Y.H., Jenkins, T.L., Selly, S.L.C., Martin,
848 S.A.M., Stevens, J.R., Santos, E.M., Davie, A., Robledo, D., 2020. Harnessing genomics to fast-track
849 genetic improvement in aquaculture. *Nat Rev Genet* 21(7), 389-409. [https://doi.org/10.1038/s41576-
850 020-0227-y](https://doi.org/10.1038/s41576-020-0227-y)
851 Hu, Y.M., Li, Q., Xu, C.X., Liu, S.K., Kong, L.F., Yu, H., 2022. Genetic variability of mass-selected and wild
852 populations of Iwagaki oyster (*Crassostrea nippona*) revealed by microsatellites and mitochondrial COI
853 sequences. *Aquaculture* 561. <https://doi.org/10.1016/j.aquaculture.2022.738737>
854 Jiao, W.Q., Fu, X.T., Dou, J.Z., Li, H.D., Su, H.L., Mao, J.X., Yu, Q., Zhang, L.L., Hu, X.L., Huang, X.T., Wang,
855 Y.F., Wang, S., Bao, Z.M., 2014. High-Resolution Linkage and Quantitative Trait Locus Mapping Aided
856 by Genome Survey Sequencing: Building Up An Integrative Genomic Framework for a Bivalve Mollusc.
857 *DNA Res* 21(1), 85-101. <https://doi.org/10.1093/dnares/dst043>
858 Jiao, Z.X., Tian, Y., Hu, B.Y., Li, Q., Liu, S.K., 2021. Genome Structural Variation Landscape and Its
859 Selection Signatures in the Fast-growing Strains of the Pacific Oyster, *Crassostrea gigas*. *Mar Biotechnol*
860 23(5), 736-748. <https://doi.org/10.1007/s10126-021-10060-5>
861 Jin, W., Bai, Z.Y., Fu, L.L., Zhang, G.F., Li, J.L., 2012. Genetic analysis of early growth traits of the triangle
862 shell mussel, *Hyriopsis cumingii*, as an insight for potential genetic improvement to pearl quality and
863 yield. *Aquacult Int* 20(5), 927-933. <https://doi.org/10.1007/s10499-012-9518-4>
864 Jones, D.B., Jerry, D.R., Forêt, S., Konovalov, D.A., Zenger, K.R., 2013a. Genome-Wide SNP Validation
865 and Mantle Tissue Transcriptome Analysis in the Silver-Lipped Pearl Oyster, *Pinctada maxima*. *Mar*
866 *Biotechnol* 15(6), 647-658. <https://doi.org/10.1007/s10126-013-9514-3>
867 Jones, D.B., Jerry, D.R., Khatkar, M.S., Raadsma, H.W., Zenger, K.R., 2013b. A high-density SNP genetic
868 linkage map for the silver-lipped pearl oyster, *Pinctada maxima*: a valuable resource for gene
869 localisation and marker-assisted selection. *Bmc Genomics* 14. [https://doi.org/10.1186/1471-2164-14-
870 810](https://doi.org/10.1186/1471-2164-14-810)
871 Jourdan, A., Morvezen, R., Enez, F., Haffray, P., Lange, A., Vetois, E., Allal, F., Phocas, F., Bugeon, J.,
872 Degremont, L., Boudry, P., 2023. Potential of genomic selection for growth, meat content and colour
873 traits in mixed-family breeding designs for the Pacific oyster *Crassostrea gigas*. *Aquaculture* 576.
874 <https://doi.org/10.1016/j.aquaculture.2023.739878>
875 Kriaridou, C., Tsairidou, S., Houston, R.D., Robledo, D., 2020. Genomic Prediction Using Low Density
876 Marker Panels in Aquaculture: Performance Across Species, Traits, and Genotyping Platforms. *Front*
877 *Genet* 11. <https://doi.org/10.3389/fgene.2020.00124>
878 Legarra, A., Croiseau, P., Sanchez, M.P., Teyssèdre, S., Sallé, G., Allais, S., Fritz, S., Moreno, C.R., Ricard,
879 A., Elsen, J.M., 2015. A comparison of methods for whole-genome QTL mapping using dense markers
880 in four livestock species. *Genet Sel Evol* 47. <https://doi.org/10.1186/s12711-015-0087-7>
881 Liu, J.Y., Peng, W.Z., Yu, F., Shen, Y.W., Yu, W.C., Lu, Y.S., Lin, W.H., Zhou, M.Z., Huang, Z.K., Luo, X.,
882 You, W.W., Ke, C.H., 2022. Genomic selection applications can improve the environmental
883 performance of aquatics: A case study on the heat tolerance of abalone. *Evol Appl* 15(6), 992-1001.
884 <https://doi.org/10.1111/eva.13388>
885 Lupo, C., Bougeard, S., Le Bihan, V., Blin, J.L., Allain, G., Azema, P., Benoit, F., Bechemin, C., Bernard, I.,
886 Blachier, P., 2021. Mortality of marine mussels *Mytilus edulis* and *M. galloprovincialis*: systematic

887 literature review of risk factors and recommendations for future research. *Rev Aquacult* 13(1), 504-
888 536. <https://doi.org/10.1111/raq.12484>

889 Mallet, A.L., Freeman, K.R., Dickie, L.M., 1986. The Genetics of Production Characters in the Blue
890 Mussel *Mytilus-Edulis* .1. A Preliminary-Analysis. *Aquaculture* 57(1-4), 133-140.
891 [https://doi.org/10.1016/0044-8486\(86\)90190-0](https://doi.org/10.1016/0044-8486(86)90190-0)

892 McCarty, A.J., Allen, S.K., Plough, L.V., 2022. Genome-wide analysis of acute low salinity tolerance in
893 the eastern oyster *Crassostrea virginica* and potential of genomic selection for trait improvement. *G3-
894 Genes Genomes Genetics* 12(1). <https://doi.org/10.1093/g3journal/jkab368>

895 Misztal, I., Tsuruta, S., Lourenco, D.A.L., Aguilar, I., Legarra, A., Vitezica, Z., 2014. BLUPF90 and related
896 programs (BGF90).

897 Nascimento-Schulze, J.C., Bean, T.P., Penalzoza, C., Paris, J.R., Whiting, J.R., Simon, A., Fraser, B.A.,
898 Houston, R.D., Bierne, N., Ellis, R.P., 2023. SNP discovery and genetic structure in blue mussel species
899 using low coverage sequencing and a medium density 60 K SNP-array. *Evol Appl* 16(5), 1044-1060.
900 <https://doi.org/10.1111/eva.13552>

901 Nguyen, T.T.T., Hayes, B.J., Ingram, B.A., 2014. Genetic parameters and response to selection in blue
902 mussel (*Mytilus galloprovincialis*) using a SNP-based pedigree. *Aquaculture* 420, 295-301.
903 <https://doi.org/10.1016/j.aquaculture.2013.11.021>

904 Nie, H.T., Yan, X.W., Huo, Z.M., Jiang, L.W., Chen, P., Liu, H., Ding, J.F., Yang, F., 2017. Construction of
905 a High-Density Genetic Map and Quantitative Trait Locus Mapping in the Manila clam *Ruditapes
906 philippinarum*. *Sci Rep-Uk* 7. <https://doi.org/10.1038/s41598-017-00246-0>

907 Nordio, D., Khtikian, N., Andrews, S., Bertotto, D., Leask, K., Green, T., 2021. Adaption potential of
908 *Crassostrea gigas* to ocean acidification and disease caused by *Vibrio harveyi*. *Ices J Mar Sci* 78(1), 360-
909 367. <https://doi.org/10.1093/icesjms/fsaa080>

910 Norman, R.A., Crumlish, M., Stetkiewicz, S., 2019. The importance of fisheries and aquaculture
911 production for nutrition and food security. *Rev Sci Tech Oie* 38(2), 395-407.
912 <https://doi.org/10.20506/rst.38.2.2994>

913 Normand, J., Benabdelmouna, A., Louis, W., Grizon, J., 2022. MYTILOBS Campagne 2020-2021. Réseau
914 d'observation des moules d'élevage sur la côte Atlantique et dans la Manche. Edition 2022.

915 Odegård, J., Moen, T., Santi, N., Korsvoll, S.A., Kjøglum, S., Meuwissen, T.H.E., 2014. Genomic
916 prediction in an admixed population of Atlantic salmon (*Salmo salar*). *Front Genet* 5.
917 <https://doi.org/10.3389/fgene.2014.00402>

918 Oden, E., Burioli, E.A.V., Trancart, S., Pitel, P.H., Houssin, M., 2016. Multilocus sequence analysis of
919 *Vibrio splendidus* related-strains isolated from blue mussel *Mytilus* sp during mortality events.
920 *Aquaculture* 464, 420-427. <https://doi.org/10.1016/j.aquaculture.2016.07.024>

921 Oikonomou, S., Samaras, A., Tekeoglou, M., Loukovitis, D., Dimitroglou, A., Kottaras, L., Papanna, K.,
922 Papaharisis, L., Tsigenopoulos, C.S., Pavlidis, M., Chatziplis, D., 2022. Genomic Selection and Genome-
923 Wide Association Analysis for Stress Response, Disease Resistance and Body Weight in European
924 Seabass. *Animals-Basel* 12(3). <https://doi.org/10.3390/ani12030277>

925 Palaiokostas, C., Ferrarresso, S., Franch, R., Houston, R.D., Bargelloni, L., 2016. Genomic Prediction of
926 Resistance to Pasteurellosis in Gilthead Sea Bream (*Sparus aurata*) Using 2b-RAD Sequencing. *G3-
927 Genes Genomes Genetics* 6(11), 3693-3700. <https://doi.org/10.1534/g3.116.035220>

928 Palaiokostas, C., Vesely, T., Kocour, M., Prchal, M., Pokorova, D., Piackova, V., Pojezdal, L., Houston,
929 R.D., 2019. Optimizing Genomic Prediction of Host Resistance to Koi Herpesvirus Disease in Carp. *Front
930 Genet* 10. <https://doi.org/10.3389/fgene.2019.00543>

931 Penalzoza, C., Barria, A., Papadopoulou, A., Hooper, C., Preston, J., Green, M., Helmer, L., Kean-
932 Hammerson, J., Nascimento-Schulze, J.C., Minardi, D., Gundappa, M.K., Macqueen, D.J., Hamilton, J.,
933 Houston, R.D., Bean, T.P., 2022. Genome-Wide Association and Genomic Prediction of Growth Traits
934 in the European Flat Oyster (*Ostrea edulis*). *Front Genet* 13.
935 <https://doi.org/10.3389/fgene.2022.926638>

936 Pino-Querido, A., Alvarez-Castro, J.M., Guerra-Varela, J., Toro, M.A., Vera, M., Pardo, B.G., Fuentes, J.,
937 Blanco, J., Martinez, P., 2015. Heritability estimation for okadaic acid algal toxin accumulation, mantle

938 color and growth traits in Mediterranean mussel (*Mytilus galloprovincialis*). *Aquaculture* 440, 32-39.
939 <https://doi.org/10.1016/j.aquaculture.2015.01.032>

940 Polsenaere, P., Soletchnik, P., Le Moine, O., Gohin, F., Robert, S., Pepin, J.F., Stanisiere, J.Y., Dumas, F.,
941 Bechemin, C., Gouletquer, P., 2017. Potential environmental drivers of a regional blue mussel mass
942 mortality event (winter of 2014, Breton Sound, France). *J Sea Res* 123, 39-50.
943 <https://doi.org/10.1016/j.seares.2017.03.005>

944 Prou, J., Gouletquer, P., 2002. The French mussel industry: present status and perspectives. *Bulletin*
945 *of the Aquaculture Association of Canada* 102(3), 17-23.

946 Putnam, J.G., Steiner, J.N., Richard, J.C., Leis, E., Goldberg, T.L., Dunn, C.D., Agbalog, R., Knowles, S.,
947 Waller, D.L., 2023. Mussel mass mortality in the Clinch River, USA: metabolomics detects affected
948 pathways and biomarkers of stress. *Conserv Physiol* 11(1). <https://doi.org/10.1093/conphys/coad074>

949 Qi, H.G., Song, K., Li, C.Y., Wang, W., Li, B.S., Li, L., Zhang, G.F., 2017. Construction and evaluation of a
950 high-density SNP array for the Pacific oyster (*Crassostrea gigas*). *Plos One* 12(3).
951 <https://doi.org/10.1371/journal.pone.0174007>

952 Regan, T., Bean, T.P., Ellis, T., Davie, A., Carboni, S., Migaud, H., Houston, R.D., 2021. Genetic
953 improvement technologies to support the sustainable growth of UK aquaculture. *Rev Aquacult* 13(4),
954 1958-1985. <https://doi.org/10.1111/raq.12553>

955 Ren, P., Peng, W.Z., You, W.W., Huang, Z.K., Guo, Q., Chen, N., He, P.R., Ke, J.W., Gwo, J.C., Ke, C.H.,
956 2016. Genetic mapping and quantitative trait loci analysis of growth-related traits in the small abalone
957 *Haliotis diversicolor* using restriction-site-associated DNA sequencing. *Aquaculture* 454, 163-170.
958 <https://doi.org/10.1016/j.aquaculture.2015.12.026>

959 Rey-Campos, M., Moreira, R., Gerdol, M., Pallavicini, A., Novoa, B., Figueras, A., 2019. Immune
960 Tolerance in *Mytilus galloprovincialis* Hemocytes After Repeated Contact With *Vibrio splendidus*. *Front*
961 *Immunol* 10. <https://doi.org/10.3389/fimmu.2019.01894>

962 Robledo, D., Matika, O., Hamilton, A., Houston, R.D., 2018. Genome-Wide Association and Genomic
963 Selection for Resistance to Amoebic Gill Disease in Atlantic Salmon. *G3-Genes Genomes Genetics* 8(4),
964 1195-1203. <https://doi.org/10.1534/g3.118.200075>

965 Siol, M., Jacquin, F., Chabert-Martinello, M., Smykal, P., Le Paslier, M.C., Aubert, G., Burstin, J., 2017.
966 Patterns of Genetic Structure and Linkage Disequilibrium in a Large Collection of Pea Germplasm. *G3-*
967 *Genes Genomes Genetics* 7(8), 2461-2471. <https://doi.org/10.1534/g3.117.043471>

968 Smietanka, B., Burzynski, A., Hummel, H., Wenne, R., 2014. Glacial history of the European marine
969 mussels *Mytilus*, inferred from distribution of mitochondrial DNA lineages. *Heredity* 113(3), 250-258.
970 <https://doi.org/10.1038/hdy.2014.23>

971 Smits, M., Enez, F., Ferrareso, S., Dalla Rovere, G., Vetois, E., Auvray, J.F., Genestout, L., Mahla, R.,
972 Arcangeli, G., Paillard, C., Haffray, P., Bargelloni, L., 2020. Potential for Genetic Improvement of
973 Resistance to *Perkinsus olseni* in the Manila Clam, *Ruditapes philippinarum*, Using DNA Parentage
974 Assignment and Mass Spawning. *Front Vet Sci* 7. <https://doi.org/10.3389/fvets.2020.579840>

975 Song, H., Guo, X.M., Sun, L.N., Wang, Q.H., Han, F.M., Wang, H.Y., Wray, G.A., Davidson, P., Wang, Q.,
976 Hu, Z., Zhou, C., Yu, Z.L., Yang, M.J., Feng, J., Shi, P., Zhou, Y., Zhang, L.B., Zhang, T., 2021. The hard
977 clam genome reveals massive expansion and diversification of inhibitors of apoptosis in *Bivalvia*. *Bmc*
978 *Biol* 19(1). <https://doi.org/10.1186/s12915-020-00943-9>

979 Song, H.L., Dong, T., Yan, X.Y., Wang, W., Tian, Z.H., Sun, A., Dong, Y., Zhu, H., Hu, H.X., 2022. Genomic
980 selection and its research progress in aquaculture breeding. *Rev Aquacult*.
981 <https://doi.org/10.1111/raq.12716>

982 Soon, T.K., Ransangan, J., 2019. Extrinsic Factors and Marine Bivalve Mass Mortalities: An Overview. *J*
983 *Shellfish Res* 38(2), 223-232. <https://doi.org/10.2983/035.038.0202>

984 Suplicy, F.M., 2020. A review of the multiple benefits of mussel farming. *Rev Aquacult* 12(1), 204-223.
985 <https://doi.org/10.1111/raq.12313>

986 Tan, K., Zhang, H.K., Zheng, H.P., 2020. Selective breeding of edible bivalves and its implication of global
987 climate change. *Rev Aquacult* 12(4), 2559-2572. <https://doi.org/10.1111/raq.12458>

988 Team, P., 2024. RStudio: Integrated Development Environment for R. Posit Software, PBC, Boston, MA.
989 URL.

990 Toro, J.E., Alcapán, A.C., Ojeda, J.A., Vergara, A.M., 2004a. Selection response for growth rate (shell
991 height and live weight) in the Chilean blue mussel (*Mytilus chilensis* Hupe 1854). *J Shellfish Res* 23(3),
992 753-757.

993 Toro, J.E., Alcapán, A.C., Vergara, A.M., Ojeda, J.A., 2004b. Heritability estimates of larval and spat shell
994 height in the Chilean blue mussel (*Mytilus chilensis* Hupe 1854) produced under controlled laboratory
995 conditions. *Aquac Res* 35(1), 56-61. <https://doi.org/10.1111/j.1365-2109.2004.00985.x>

996 Tsai, H.Y., Hamilton, A., Tinch, A.E., Guy, D.R., Gharbi, K., Stear, M.J., Matika, O., Bishop, S.C., Houston,
997 R.D., 2015. Genome wide association and genomic prediction for growth traits in juvenile farmed
998 Atlantic salmon using a high density SNP array. *Bmc Genomics* 16. [https://doi.org/10.1186/s12864-
999 015-2117-9](https://doi.org/10.1186/s12864-015-2117-9)

1000 Tsuruta, S., Miszta, I., 2006. THRGIBBS1F90 for estimation of variance components with threshold and
1001 linear models. *J Anim Sci* 84, 15-15.

1002 VanRaden, P.M., 2008. Efficient Methods to Compute Genomic Predictions. *J Dairy Sci* 91(11), 4414-
1003 4423. <https://doi.org/10.3168/jds.2007-0980>

1004 Vendrami, D.L.J., Houston, R.D., Gharbi, K., Telesca, L., Gutierrez, A.P., Gurney-Smith, H., Hasegawa,
1005 N., Boudry, P., Hoffman, J.I., 2019. Detailed insights into pan-European population structure and
1006 inbreeding in wild and hatchery Pacific oysters (*Crassostrea gigas*) revealed by genome-wide SNP data.
1007 *Evol Appl* 12(3), 519-534. <https://doi.org/10.1111/eva.12736>

1008 Vera, M., Maroso, F., Wilmes, S.B., Hermida, M., Blanco, A., Fernández, C., Groves, E., Malham, S.K.,
1009 Bouza, C., Robins, P.E., Martínez, P., Consortium, C., 2022. Genomic survey of edible cockle
1010 (*Cerastoderma edule*) in the Northeast Atlantic: A baseline for sustainable management of its wild
1011 resources. *Evol Appl* 15(2), 262-285. <https://doi.org/10.1111/eva.13340>

1012 Vu, S.V., Gondro, C., Nguyen, N.T.H., Gilmour, A.R., Tearle, R., Knibb, W., Dove, M., Vu, I.V., Khuong,
1013 L.D., O'Connor, W., 2021. Prediction Accuracies of Genomic Selection for Nine Commercially Important
1014 Traits in the Portuguese Oyster (*Crassostrea angulata*) Using DArT-Seq Technology. *Genes* 12(2).
1015 <https://doi.org/10.3390/genes12020210>

1016 Wang, J.P., Li, L., Zhang, G.F., 2016. A High-Density SNP Genetic Linkage Map and QTL Analysis of
1017 Growth-Related Traits in a Hybrid Family of Oysters (*Crassostrea gigas* * *Crassostrea angulata*) Using
1018 Genotyping-by-Sequencing. *G3-Genes Genomes Genetics* 6(5), 1417-1426.
1019 <https://doi.org/10.1534/g3.116.026971>

1020 Wang, Y.F., Sun, G.D., Zeng, Q.F., Chen, Z.H., Hu, X.L., Li, H.D., Wang, S., Bao, Z.M., 2018. Predicting
1021 Growth Traits with Genomic Selection Methods in Zhikong Scallop (*Chlamys farreri*). *Mar Biotechnol*
1022 20(6), 769-779. <https://doi.org/10.1007/s10126-018-9847-z>

1023 Wang, Z.Y., Hu, H.H., Sun, T.Y., Li, X., Lv, G.L., Bai, Z.Y., Li, J.L., 2022. Genomic selection for improvement
1024 of growth traits in triangle sail mussel (*Hyriopsis cumingii*). *Aquaculture* 561.
1025 <https://doi.org/10.1016/j.aquaculture.2022.738692>

1026 Yáñez, J.M., Barría, A., López, M.E., Moen, T., Garcia, B.F., Yoshida, G.M., Xu, P., 2023. Genome-wide
1027 association and genomic selection in aquaculture. *Rev Aquacult* 15(2), 645-675.
1028 <https://doi.org/10.1111/raq.12750>

1029 Yang, B., Zhai, S.Y., Zhang, F.Q., Wang, H.B., Ren, L.T., Li, Y.J., Li, Q., Liu, S.K., 2022. Genome-wide
1030 association study toward efficient selection breeding of resistance to *Vibrio alginolyticus* in Pacific
1031 oyster, *Crassostrea gigas*. *Aquaculture* 548. <https://doi.org/10.1016/j.aquaculture.2021.737592>

1032 Zenger, K.R., Khatkar, M.S., Jones, D.B., Khalilisamani, N., Jerry, D.R., Raadsma, H.W., 2019. Genomic
1033 Selection in Aquaculture: Application, Limitations and Opportunities With Special Reference to Marine
1034 Shrimp and Pearl Oysters. *Front Genet* 9. <https://doi.org/10.3389/fgene.2018.00693>

1035 Zhai, S.Y., Yang, B., Zhang, F.Q., Li, Q., Liu, S.K., 2021. Estimation of genetic parameters for resistance
1036 to *Vibrio alginolyticus* infection in the Pacific oyster (*Crassostrea gigas*). *Aquaculture* 538.
1037 <https://doi.org/10.1016/j.aquaculture.2021.736545>

1038

1039

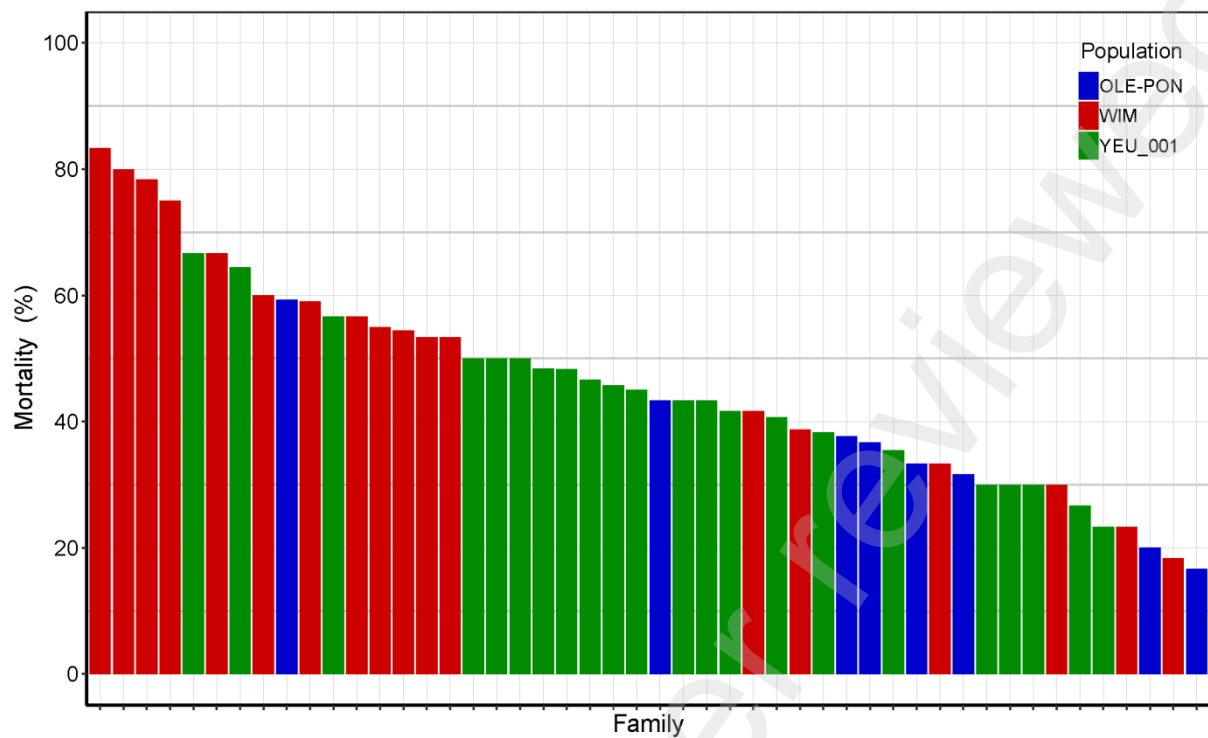


Figure 1: Final cumulative mortality 72 hours post-injection for each family. Each bar represents a family and each color represent a population.

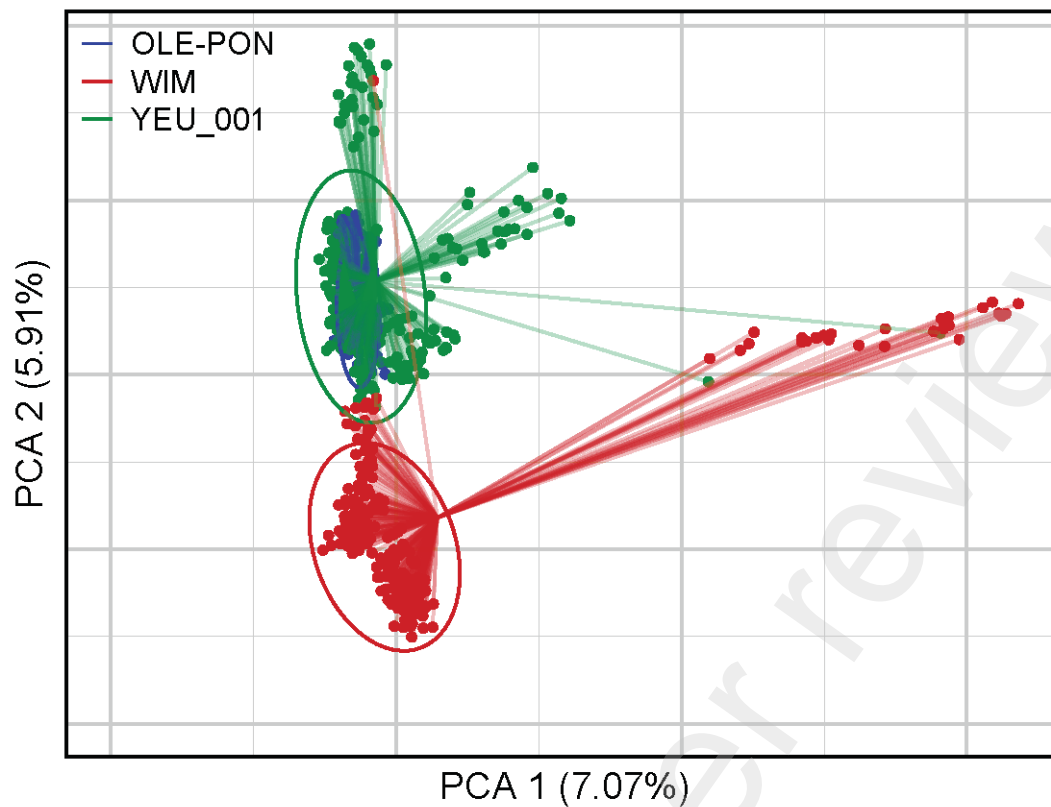


Figure 2: First two axes and associated variances of the principal component analysis (PCA) of the genetic diversity among the three populations of *Mytilus edulis*. The ellipses are constructed with axes defined as 1.5 times the standard deviation of the projections of individual coordinates on the axes. PCA was performed with 644 individuals and 3096 SNPs.

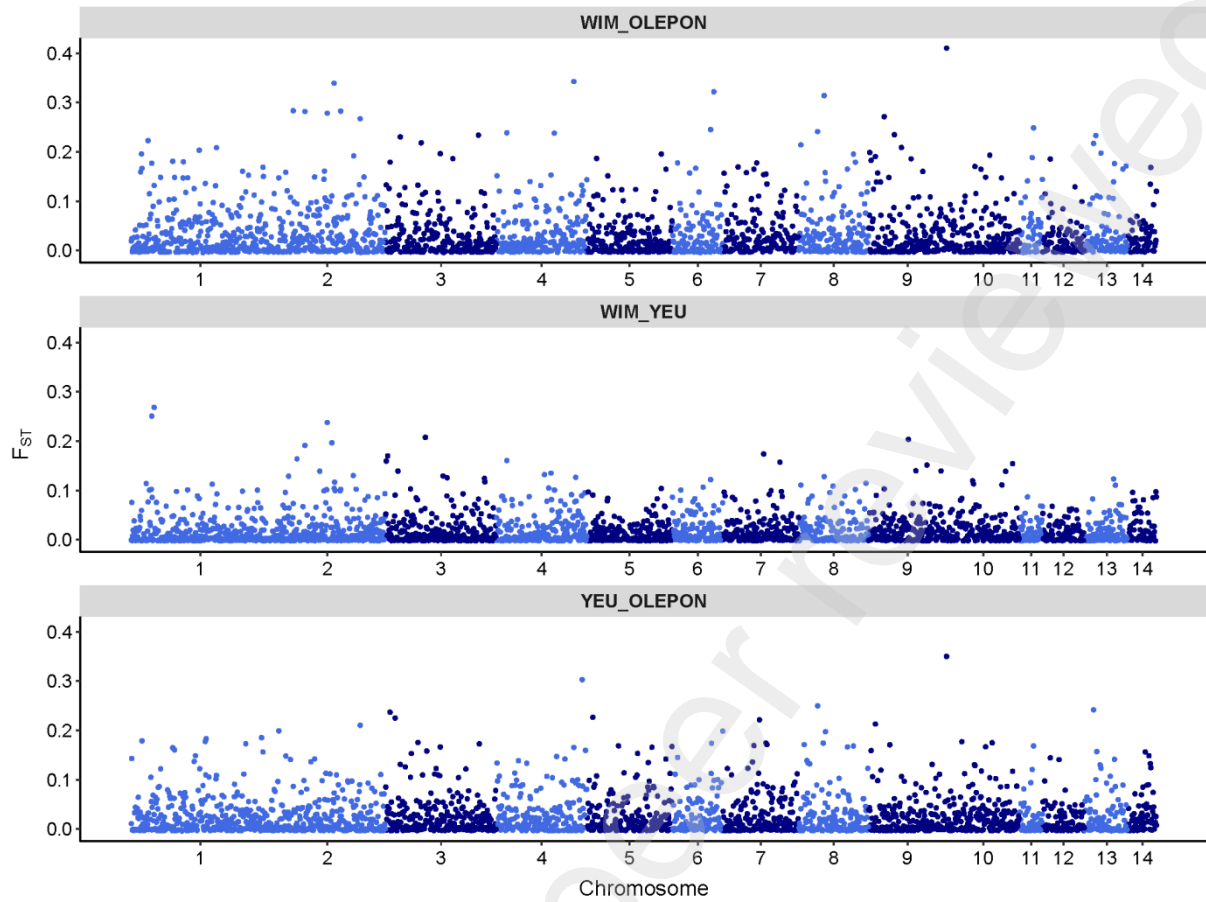


Figure 3: Genomic distribution of fixation index (F_{ST}) values as a function of chromosome position in the mussel genome for different studied population

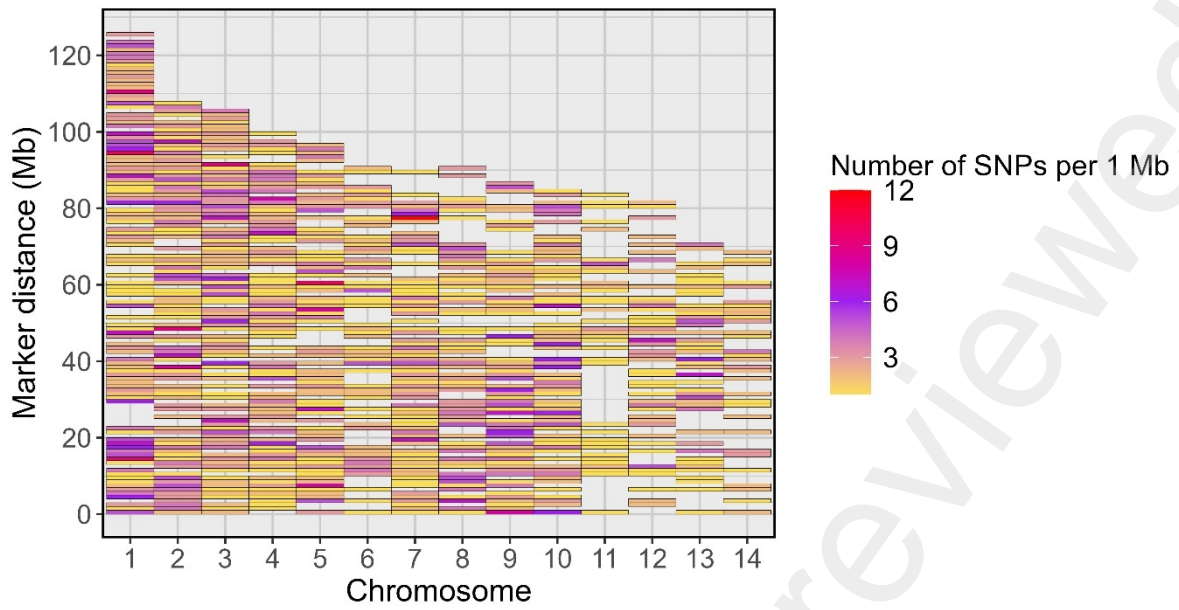


Figure 4: Identification of high-quality SNPs and their distribution across the 14 chromosomes of *M. edulis*. The gradient colors from yellow to red denote the increase of SNP density within 1 Mb interval.

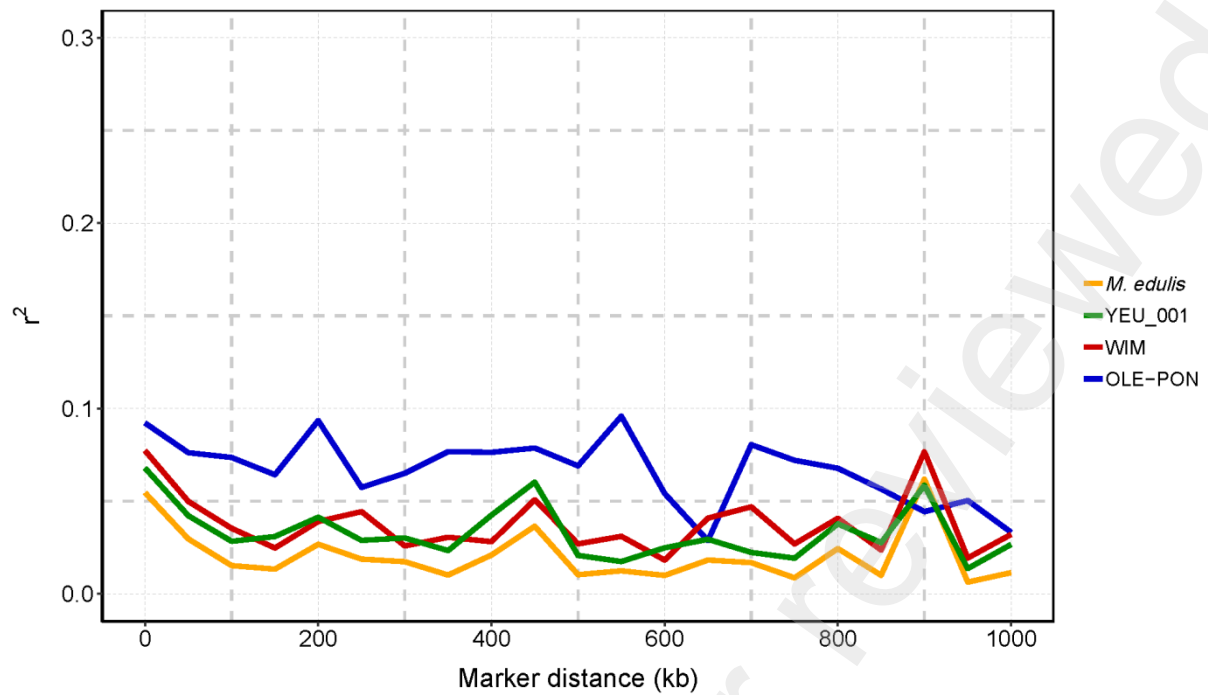


Figure 5: Linkage disequilibrium (r^2) decay with physical distance between markers in each population and overall challenged to *V. splendidus*. The X-axis is the physical location, and the Y-axis is the linkage disequilibrium value (r^2).

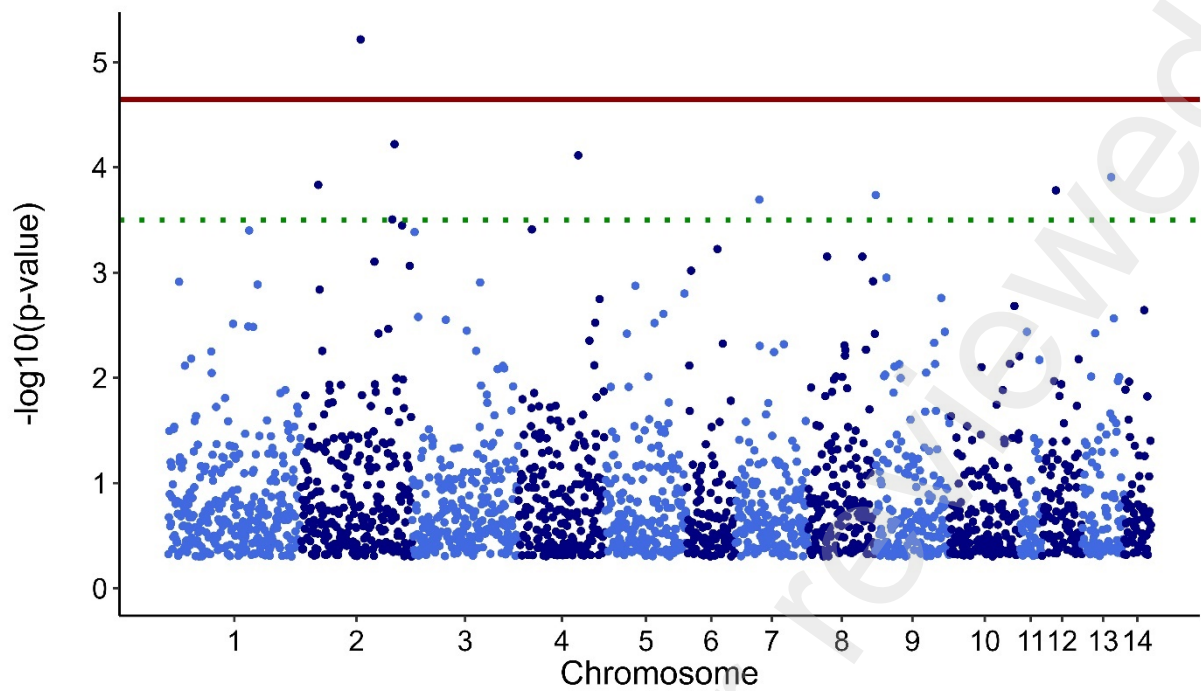


Figure 6: Manhattan plot of GWAS with p-values distributed across different chromosomes. Horizontal red line represents the 5% genome-wide significance threshold and the green line is the 5% chromosome-wide significance threshold calculated with the Bonferroni correction.

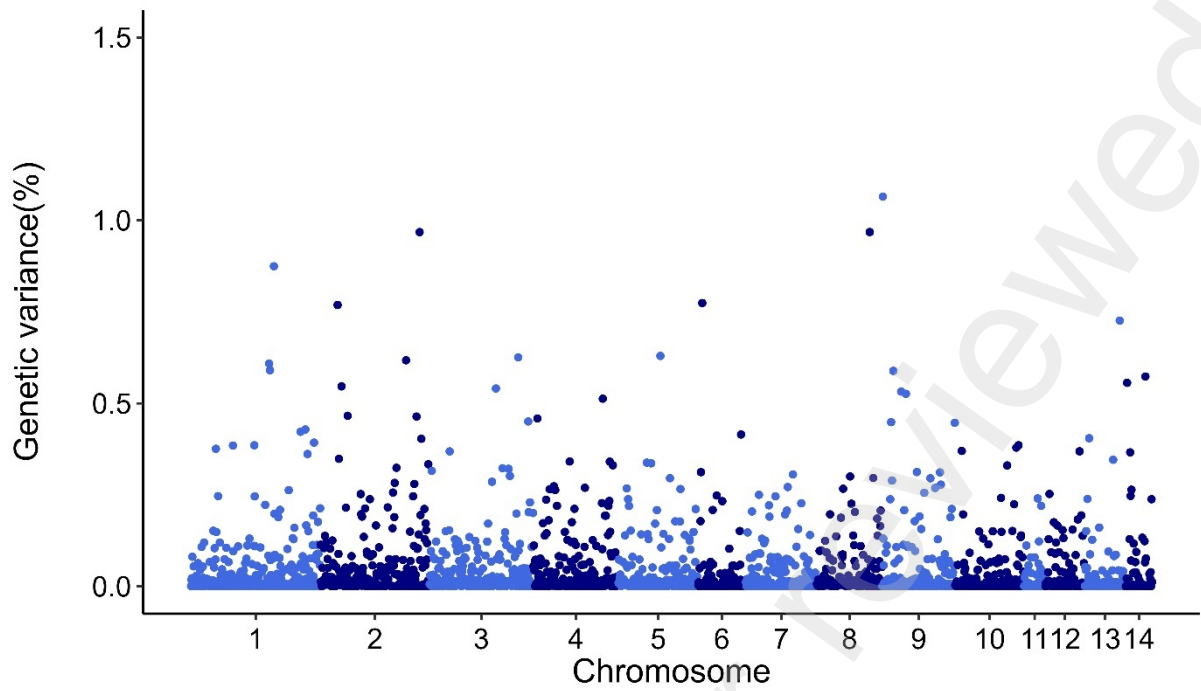


Figure 7: Manhattan plot of genetic variance explained by each SNP for resistance to *V. splendidus* in *M. edulis* using ssGBLUP approach. In X axis SNP per chromosome and Y axis percentage of genetic variance explained per each SNP.

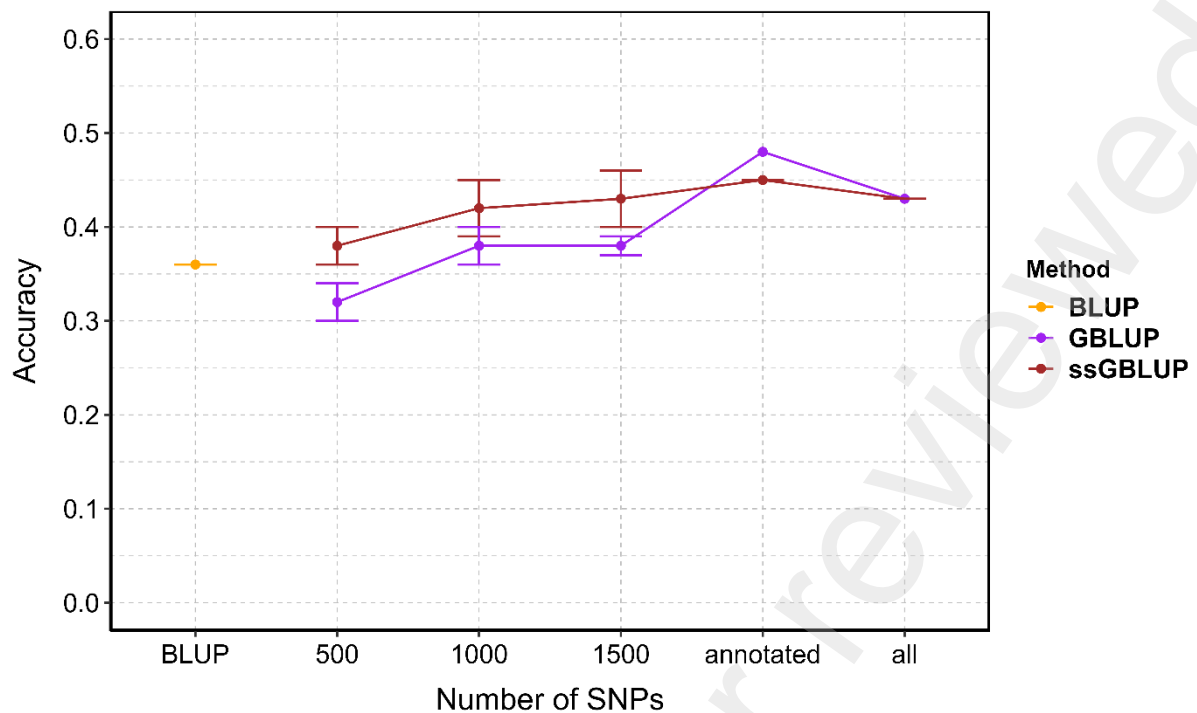


Figure 8: The estimated prediction accuracy of *Vibrio splendidus* resistance in *Mytilus edulis* using PBLUP, GBLUP and ssGBLUP across different marker densities. Each point is the average of 5 replicates. Error bars represent the standard error of the mean of 5 replicates. PBLUP - Pedigree based breeding values using all phenotyped animals, respectively. GBLUP - Genomic breeding values from only genotype animals, and ssGBLUP - Genomic breeding values from all genotyped and phenotyped animals obtained with a combined relationship matrix (H).

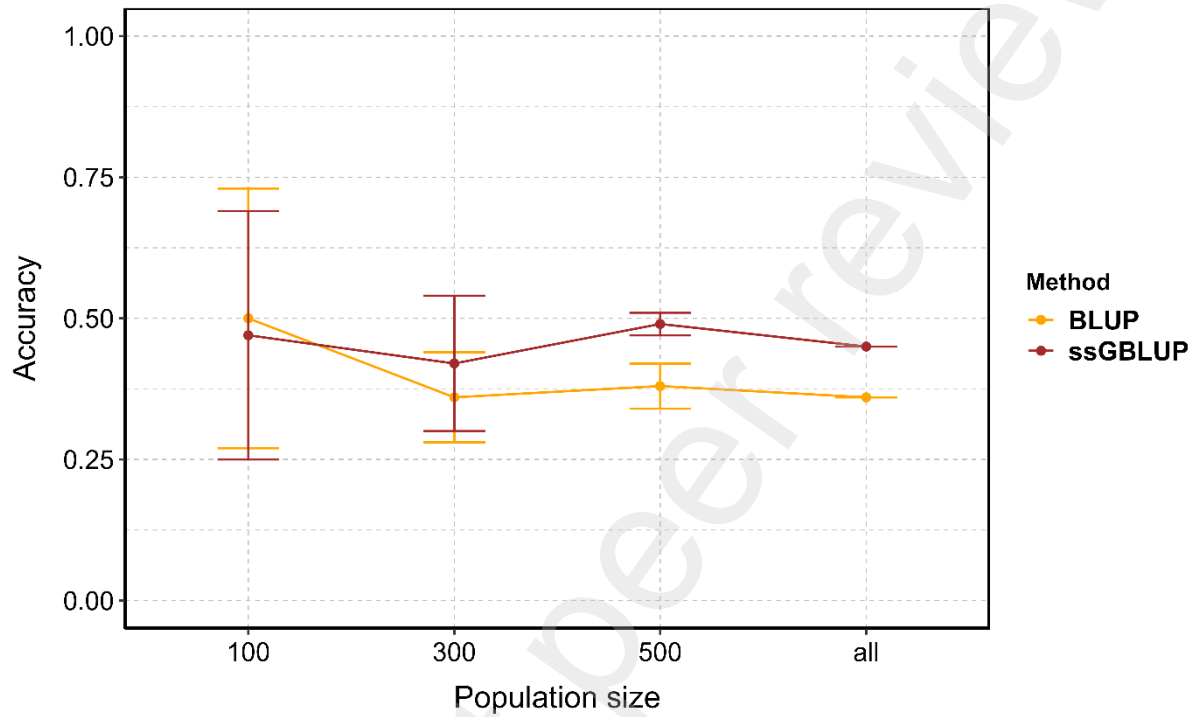


Figure 9: The estimated prediction accuracy of *Vibrio splendidus* resistance in *Mytilus edulis* using different training population size and fixed SNP density (annotated SNPs, ~2,400). Each point is the average of 5 replicates. Error bars represent the standard error of the mean of 5 replicates.

Table 1: Summary of the experimental infection using the pathogenic strain 14/053 2T1 of *Vibrio splendidus* in *Mytilus edulis*

	Phenotyped	Genotyped
Number of families	48	48
Total number of mussels	2160	768
Mean number of mussels/family	45	14.5 (Min:13; Max:16)
Mean mortality	47.3%	50%

Table 2: Pairwise FST between populations of *Mytilus edulis*

	WIM	YEU_001
OLE-PON	0.03	0.03
WIM		0.02

Table 3: Variance components and genetics parameters for *V. splendidus* resistance in *M. edulis*

Method	Model	Relationship matrix	h^2 (\pm se)
PBLUP	Linear	A	0.22 (0.06)
	Gibbs sampling	A	0.31 (0.05)
GBLUP	Linear	G	0.33 (0.11)
	Gibbs sampling	G	0.36 (0.05)
ssGBLUP	Linear	H	0.28 (0.08)
	Gibbs sampling	H	0.33 (0.05)

σ_a^2 : Additive genetic variance; σ_e^2 : Residual variance; σ_p^2 : Phenotypic variance; A: Pedigree based relationship matrix; G: Genomic based relationship matrix; H: genomic and pedigree combined relationship matrix; Linear: Linear mixed model; h^2 : heritability. The h^2 for linear model on observed scale transferred into underlying scale using the formulae from Dempster and linear (1950).

Table 4: The significant SNPs detected in GWAS analysis (ssGBLUP) ranked with respect to level of significance. Position = Physical position of SNP on the chromosome; A1 & A2 = Minor & major alleles, respectively; MAF = Minor allele frequency; P = Significance value; varG = percentage of genetic variance explained by SNP

SNP_ID	Chromosome	Position	A1	A2	MAF	P-value	VarG (%)
AX-604335979	2	61,614,609	A	C	0.07	5.21	0.10
AX-603804982	2	91,444,473	A	T	0.04	4.22	0.04
AX-604452846	4	74,391,047	C	T	0.04	4.11	0.04
AX-603077107	13	50,001,059	A	T	0.11	3.9	0.04
AX-604514378	2	12,942,241	T	C	0.25	3.83	0.77
AX-604131039	12	33,942,361	G	A	0.06	3.79	0.09
AX-604710899	9	3,56,838	A	T	0.32	3.74	1.06
AX-604289929	7	30,079,060	C	T	0.09	3.64	0.22